CRC for
Water Sensitive Cities

Performance of two urban stormwater biofilters in an area with seasonally high groundwater

Carlos Ocampo (UWA), Bronwyn Rennie (DoW)
& Carolyn Oldham (UWA)

Australian Government
Department of Industry and Science

Business
Cooperative Research
Centres Programme

Performance of two urban stormwater biofilters in an area with seasonally high groundwater
Hydrology and nutrient transport processes in groundwater – surface water systems
(Project B2.4) B2.4-1-2016

Authors

Carlos Ocampo (UWA), Bronwyn Rennie (DoW), Carolyn Oldham (UWA)

ISBN: 978-1-921912-39-9

Publisher

Cooperative Research Centre for Water Sensitive Cities

Level 1, 8 Scenic Blvd, Clayton Campus
Monash University
Clayton, VIC 3800

p. +61 3 9902 4985
e. admin@crcwsc.org.au
w. www.watersensitivecities.org.au

Date of publication: February 2017

An appropriate citation for this document is:

Ocampo et al. (2017) Performance of two urban stormwater biofilters in an area with seasonally high groundwater. Melbourne, Australia: Cooperative Research Centre for Water Sensitive Cities.

Acknowledgments

Fieldwork was undertaken by The University of Western Australia and the Department of Water of Western Australia (DoW) under the project “Evaluation of Urban Stormwater Best Management Practices”. This project was funded by the CRC Water Sensitive Cities, and the Western Australian Government’s Natural Resource Management program. The Department of Parks and Wildlife supported this project under the Swan-Canning Water Quality Improvement Plan. Fieldwork activities were supported by Ryan Kam (DoW) and James Hehre, Kellie Van Hees and David Van Brocklin (UWA).

Table of Contents

List of Figures

List of Tables

Executive Summary

Biofilters are used in urban areas throughout the world to attenuate storm flows and stormwater nutrient loads. Many urban developments on the Swan Coastal Plain in Western Australia experience a seasonally high water table; when the water table intercepts the biofilters it is more challenging to determine the consequences for biofilter performance. This report sets out methods for assessing performance of two biofilters (a raingarden and a bioretention basin) over a year that included the high water table conditions, quantifies both the hydrological and nutrient removal performance of the two systems, and makes recommendations for improved performance. Specifically, we aimed to:

- *quantify the effectiveness of each type of biofilter in reducing runoff volumes and peaks,*
- *quantify the nutrient removal performance of each of the biofilters,*
- *quantify the effect high groundwater has on each of the biofilter's hydrological functioning and nutrient removal performance, and*
- *quantify any changes in nutrient concentrations and speciation from the inflows to the outflows.*

The study site was within The Glades development, a residential area located at the base of the Darling Scarp, approximately 2 km south west of the Byford town centre, Perth, Western Australia. The median strip raingarden and the bioretention basin were part of a series of structural controls to treat stormwater before discharging into Cardup Brook Tributary 6, which is a surface water tributary of the Peel-Harvey estuary. The shallow soil consists of sands overlying hardpan layers (locally known as duplex soils) that can create seasonally perched shallow water tables. The regional water table typically rises over winter to incorporate the perched layers into a continuous saturated soil profile. In below-average rainfall years the lower recharge may maintain the regional water table below the perched shallow water table.

Hydrological performance of the biofilters

The volumetric and peak flow reduction of the raingarden was excellent. The raingarden achieved an average event volume retention of 68%, ranging from 24-99% depending on storm size and antecedent conditions. Volumetric control by the raingarden under wet conditions for major events was 29% on average and similar to the average value reported in the literature (Hatt et al., 2009). The reduction in peak flow was 89% across the season and a minimum of 80%. Small runoff events are completely absorbed by the raingarden, which required a minimum of a 10 mm event to generate outflow. The saturated hydraulic conductivity of the filter media was high and was able to handle a flow rate of up to 5 L/s.

The excellent hydrological performance of the raingarden indicates that its physical dimensions (40 m x 4.5 m) were proportioned appropriately for the catchment size and that the filter media was able to retain volume and allow infiltration to surrounding soils (estimated at 38% of the annual water input).

There was no direct interaction between the water table and the raingardens outflow pipes. While the perched groundwater did not discharge directly into the raingarden, as the water table rose over the season, the infiltration rate from the raingarden decreased. Also, the water table was well above the invert of all the stormwater pits at Mead Street (Section 2.1) and was effectively contributing to the flow of the main drainage network and intercepted the bioretention basin outflow pipe. This impacted both hydrological performance and nutrient attenuation in the bioretention basin.

Because of the water table interception, careful consideration of rainfall event characteristics and antecedent conditions was necessary to interpret hydrologic efficiency in the bioretention basin. An average volume reduction of approximately 16% was achieved for rainfall events close to design conditions (1-year ARI, 1 hr duration). High water table levels in the area at the time of the monitored events likely reduced infiltration and groundwater contributed to the outflow.

The hydrological performance of the bioretention basin for smaller events (5-14 mm) was dependent on season and overall achieved the design volumetric reduction; by October the water table dropped below the subsurface drainage pipes, and subsequent volume reduction for these small events reached 50%.

Nutrient treatment performance of the biofilters

Nutrient attenuation was quantified by comparing nutrient concentrations and nutrient loads for the inflows and outflows. Water samples were collected for inflows and outflows across rainfall events and later analysed for nutrient concentrations. During rainfall events water samples were collected with 2-bottle auto-sampling, surface water runoff traps, and complemented with manual grab sampling. Nutrient loads were estimated as the product of nutrient concentrations and the inflow/outflow discharges.

Over the season, the raingarden was highly effective at total phosphorus (TP) load attenuation (up to 90%). This is likely due to efficient removal of suspended solids from the stormwater, as well as the volume reduction across the raingarden. The filterable reactive phosphorus (FRP) load attenuation was on average 72%. Over the season, the raingarden attenuated total nitrogen (TN) load well (mean 86%). However it appears to be ineffective at treating nitrate (NOx-N). This is likely to be due to the lack of a saturated or submerged zone to provide anoxic conditions for denitrification, whereby nitrates can be broken down. Another factor contributing to the low nitrate load attenuation may be the short residence time of the water through the filtering soil media; this reduces the time NOx-N is exposed to nitrate-reducing microorganisms and plant uptake.

The dynamics of the bioretention basin were more complex than the raingarden, and it exhibited strong seasonality related to the interception of the water table around August. During this period, the high water table contributed up to 20% of the outflows and storm flow attenuation decreased (the water volume reductions were 10% and 40% for major and minor rainfall events respectively). The interception of the water table also impacted the nutrient attenuation dynamics; event average (during the flow season) TN and TP load attenuations of 30-40% were considerably lower than measured at the raingarden.

Both the raingarden and the bioretention basin consistently attenuated phosphorus loads more effectively than nitrogen loads. Particulate phosphorus made up a significant proportion of TP and was effectively trapped by both systems. Both systems were well oxygenated and under those conditions the filter media was effective at attenuating FRP loads.

The nitrogen dynamics were more complex. While TN loads were on average attenuated by both systems, there was variability across the year and they exhibited periods of lower attenuation of NOx-N. This was likely due to the toxic conditions that were maintained in the filter media. In the bioretention basin, these oxic conditions were likely maintained by the short travel times of sub-surface drain inflows.

Ideally biofilters provide a range of redox conditions for optimal nutrient attenuation; this occurs readily in systems with lower permeability soils and higher organic matter content that experience frequent rainfall throughout the year. Biofilters installed in urban areas in Perth experience hot and dry summers, a water table and high permeability soils. These maintain oxic conditions in the biofilter media during the summer season. Winter rains and higher water tables may increase the degree of surface soil saturation, however the high soil permeability and short sub-surface travel times (exacerbated by sub-surface drainage) inject oxygen into the system.

This oxygen dynamic and resulting redox conditions have a profound impact on phosphorus and nitrogen attenuation; phosphorus is attenuated effectively under oxic conditions while nitrogen is not. When a single system (whether a raingarden or a bioretention basin) aims for attenuation of both nitrogen and phosphorus, there will always be challenges in how to maintain the optimal redox conditions. We recommend that:

1. *A treatment train approach is used across the catchment, to provide a range of redox conditions for nutrient attenuation. Consider alternating surface and sub-surface treatment trains across the catchment.*

2. *Design systems to extend the travel time of sub-surface flows across the catchment, and through the filter media. This has to be balanced with the required volume attenuation; hydrological and hydraulic modelling is critical to optimise this performance.*

3. *Consider the placement of smaller biofilters throughout the catchment, including in the upland areas, to increase infiltration, water table development and consequently sub-surface travel times and increase the likelihood of nutrient attenuation.*

1. Introduction

1.1 Background

Biofilters are structural water sensitive urban design (WSUD) elements that use physical and biological processes to treat stormwater. They are one of the WSUD elements considered to be best practice. They improve the hydrology of stormwater by buffering the frequent flashy flows created by impervious surfaces in urban developments, and improve water quality by removing nutrients, suspended sediment, and other pollutants. In addition they can provide attractive landscape features, habitat for wildlife, and improve the urban microclimate.

A biofilter is generally comprised of a trench or basin filled with porous filter media and then densely vegetated. Stormwater is treated as it flows through the dense vegetation, the filter media and the root zone. Pollutants are removed via a combination of physical processes (such as sedimentation and physical straining), chemical processes (such as sorption), and biological processes (such as plant and microbial uptake). Depending on the design, the treated outflow is either infiltrated to underlying soils, or collected by pipes for conveyance downstream.

Guidelines are available to assist with biofilter design (Payne et al., 2015). These guidelines were based on extensive research however the majority of these studies were done either in the laboratory or on biofilters that were isolated from groundwater. As such, there is a lack of information on how biofilters function when there is interaction with the groundwater.

Many urban developments on the Swan Coastal Plain in Perth (Western Australia) experience a high water table, which provides an additional level of complexity in the design and subsequent performance assessment of biofilters. For example, during the wet winter, the shallow water table could act as either a source or sink of nutrients, and could decrease the unsaturated zone available beneath biofilters. This would affect the hydrological and water quality performance of the biofilter.

This report evaluates two types of biofilters installed in areas with a high water table. Both biofilters were installed following best practice within the limitations of practicalities.

1.2 Aim and scope of work

The aim of this study was to help address knowledge gaps surrounding the hydrological function and nutrient removal performance of established biofilters in areas of high groundwater on the Swan Coastal Plain in Perth, WA. Two types of biofilters were assessed: a) median strips with shallow flow conditions (raingardens); and b) a surface storage facility at end of system acting as a bioretention basin. The main differences between these two systems were the inflow volumes and the runoff conditions (rapid sheet-flow versus shallow surface storage) resulting from their upstream contributing catchment; these required different monitoring and data analysis approaches.

Specifically, we set out to answer the following questions:

- What is the effectiveness of each type of biofilter in reducing runoff volumes and peaks?
- What is the nutrient removal performance of each of the biofilters?
- What effect does high groundwater have on each of the biofilters hydrological functioning and nutrient removal performance?
- What are the changes in nutrient concentrations and speciation from the inflows to the outflows?

The biofilters are located in Stage 1, The Glades development in Byford, Western Australia. The biofilters were monitored from October 2014 to October 2015 to assess performance over a full water year cycle and across rainfall events of different magnitude.

Hydrological data was used to develop a water balance model and assess biofilter hydrological performance. Water quality data was then used to determine nutrient removal performance. These assessments aim to inform future biofilter design, improve modelling tools commonly used by practitioners, and provide guidance on biofilter performance assessment in areas of high groundwater.

2. Study site and biofilters

The study site is part of The Glades development, a residential area located at the base of the Darling Scarp, approximately 2 km south west of the Byford town centre, Perth, Western Australia. Site works for the development began in mid-2008, and building construction began in 2009 with Stage 1, A and B (Figure 1) comprising a 15.3 hectare residential housing development (JDA, 2009). The biofilters were completed in 2010; they were therefore five years old during this monitoring and had well-established, mature vegetation. This was important because biofilters require an establishment period of approximately two years to settle the filter media and allow the vegetation to reach its design conditions (FAWB, 2009).

The median strip raingarden and the bioretention basin were part of a series of structural controls to treat stormwater before discharging into Tributary 6 of Cardup Brook, which is a surface water tributary of the Peel-Harvey estuary. The biofilters were designed to meet the most relevant design guidelines at the time of construction (FAWB, 2009) as much

as practicable. Instead of the recommended transition and drainage layers under the filter media, a homogenous media of Gingin loam was used, with a slotted subsoil pipe. The local Gingin loam has been found to meet the requirements of biofilter media according to FAWB (2009) and demonstrated good efficiency in contaminant removal (Seah, 2011).

The catchment area (Stage 1A) for the bioretention basin was 8.7 ha (comprising of 4.9 ha lot areas, 2.4 ha road area and 1.4 ha of public open space) (JDA, 2009) as shown in Figure 1. Impervious area directly connected (road, driveway and pathways) in Stage 1A has an average slope of 0.035 m/m, stormflow is collected by a piped network (0.225 m diameter) and discharged into the main drainage pipe at Mead Street. A series of raingardens also collected and treated surface runoff from adjacent impervious areas (roads and footpaths) each with a catchment area of 0.21 ha (see dark shaded area in Figure 1). The main stormwater drainage pipe system at Mead Street (0.9 m in diameter) has a capacity for a 5-year average recurrence interval (ARI), and discharges to a diversion structure (bubble up sump) at its end point (~400 m downstream). This allows small rainfall events (up to the 1-year ARI 1-hour duration) to flow to the bioretention basin (BF4 in Figure 1) via two 300 mm pipes. Larger flows (> 1 – 100 year ARI) are restricted by the pipe capacity and therefore diverted around the bioretention storage to an adjacent grassed storage area (Figure 1) that forms part of the public open space (JDA, 2009).

The superficial aquifer in this region is referred to as the Byford Area, and extends approximately 166 km^2. The aquifer has a maximum thickness of 20 m and consists of clayey sediments of the Guildford Clay (JDA, 2009). The deep aquifer of the region is the Cattamarra Coal (JDA, 2009). The shallow soil consists of sands overlying hardpan layers (locally known as duplex soils) that can create seasonally perched shallow water tables. The regional water table typically rises over winter to incorporate the perched layers into a continuous saturated soil profile. In below-average rainfall years the lower recharge may maintain the regional water table below the perched shallow water table (JDA, 2009).

Prior to development, the soil profile consisted of a 0.1 m thick topsoil layer overlying a 1–1.5 m thick sandy-loam material before reaching a clay layer at a depth of approximately 1.8 m (Coffey Geotechnics, 2007). To meet development requirements approximately 0.8 m of controlled fill (uniform fine sand) was applied. A subsoil drainage system was installed at a depth of 1.2 m (below ground level) to protect infrastructure from flooding and inundation by high levels of the regional or locally perching groundwater.

The area presents a Mediterranean climate characterised by dry, hot summers and wet winter seasons and has received an average annual rainfall of 859 mm and pan evaporation of 1800 mm (BOM, 2015).

Figure 1: Byford The Glades (Stage 1 A and B) series of biofilters.

2.1 The raingardens

The raingardens (BF1 and BF2) are situated in the median strip of Mead Street (Figure 1). They are vegetated swales approximately 40 m long and 4.5 m wide, with a cross-sectional area of 1.5 m^2 (Figure 2). The central median strip is an inverted crown with flush kerbing to ensure that runoff flows directly from the paved road surface into the raingarden by sheet flow (Figure 3a). The Gingin loam was used as the raingarden media (0.55 m deep) and local clay of the landscape was used to create a natural lining. The treated effluent was collected by a 0.15 m diameter slotted PVC pipe located at the base of the raingardens (JDA, 2009) and discharged into a pit joining the main drainage pipe of the area under Mead Street (Figure 3b-c).

Under major rainfall events, when the capacity of the shallow surface storage was reached, overflow gullies collected the excess stormwater and discharged it into the pit joining the main drainage pipe. The invert of the overflow gullies was set to the upper water level of the raingarden (JDA, 2009).

The raingardens were planted with drought tolerant native species that required minimal irrigation, were tolerant of periodic inundation and had a dense, spreading root system. Planting was done to ensure 70-80% coverage at plant maturity. An irrigation system was installed and used during establishment, and also during post establishment dry periods to sustain the plants and maintain landscape aesthetics. Detailed information regarding physical dimension, drainage characteristics, biofilter material, and vegetation species for the raingardens is presented in Table 1.

Figure 2: Raingarden comprising vegetated swale and flush kerb for sheet inflow. Arrows indicate flow direction.

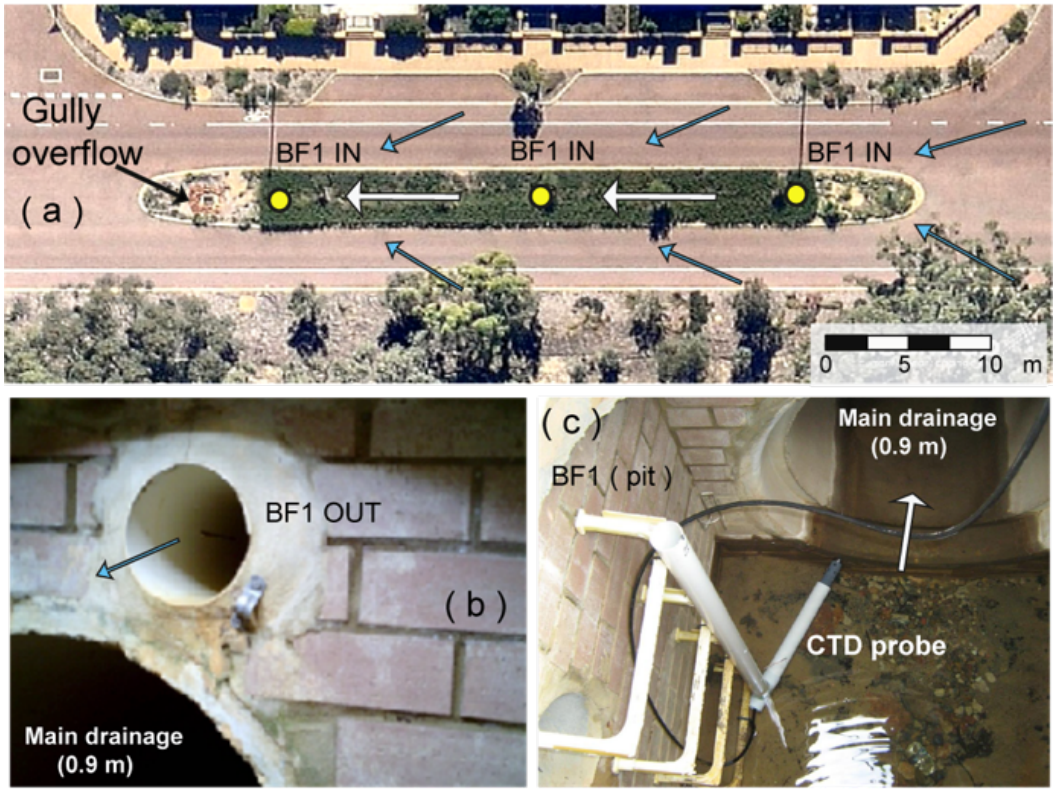

Figure 3: Raingarden drainage components and selected monitoring points; a) plan view showing inflow and sampling locations (yellow dots), b) discharging point of treated effluent, c) pit and main drainage pipe along Mead Street. Arrows indicate flow direction.

Table 1: Specifications of the raingardens

Raingardens (BF1 and BF2)	
Date of construction	2010
Filter media	Red Gingin loam (organic matter 1.16%, pH 6.12, EC 201.8, k 41.6) Minimum 500 mm thick PRI > 5 pH 5.5-7.5 Total clay and silt fraction < 3% in total (w/w) Organic matter content <5% (w/w) Phosphorus content <100 mg/kg Hydraulic Conductivity (sat) > 6 m/day. Light compaction only (JDA, 2009)
Plant species	Grevillea thelemanniana dominated Other plants included Melaleuca preissiana, and Ficinia nodosa. Flax lily (Dianella tasmanica) and grass trees (Xanthorrhoea spp) were used at the end of some of the raingardens for aesthetics
Catchment area and physical parameters	0.21 ha with an average slope of 0.027m/m collecting road runoff
Dimensions (length, width and depth)	40 x 4.5 x 0.55 m (with a 1:4 v:h sloped walls) Cross sectional area of 1.5 m^2 Storage volume of 24 kL
Lining	Lined with clay (natural soil of area)
Outlet mechanism	Slotted pipe (PVC- 0.15 m diameter, 1% slope) for subsurface media and gully overflow (into pit) for excess surface water

2.2 The bioretention basin

Stormwater from development Stage 1A and treated effluent from raingardens along Mead Street were conveyed via the main drainage pipe and directed into bioretention basin BF4 at the end of the catchment (Figure 1). The bioretention basin was sized to treat a 1-year ARI 1-hour duration event (16.9 mm hr-1) and stormwater inflows via two pipes (Ø 300 mm, 40 m long) that connected the main pit (BF4IN-BSUMP) to the BF4 basin (Figure 4b). For rainfall events in excess of this, water in the pipes backed up and formed a hydraulic head in the pit, which released stormflow through a bubble up and was then directed into the adjacent public open space (Figure 4a). The public open space served as a high flow detention basin capable of handling the 100-year ARI event (JDA, 2009). Amended soil was used as the filter media (0.5 m deep, PRI >5) to provide a saturated hydraulic conductivity of 6 m/day (Table 1).

The outlet from the bioretention basin was a series of subsurface slotted pipes that collected treated stormwater as it infiltrated through the filter media and conveyed it to a manhole (1.2 m diameter) prior to final discharge into Tributary 6 (Figure 4a,c) via a concrete pipe (Ø 300 mm). Any overflow from the basin was directed to Tributary 6 via a small spillway (using 1 m of the footpath), set 0.10 m above the designed water level for the 1-year ARI event (Figure 4a). The basin was not sealed, but was lined with the local clay from the natural landscape. Figure 5 and Figure 6 show the bioretention basin with standing water after a small rainfall event and dry conditions respectively.

Detailed information regarding physical dimensions, drainage characteristics, biofilter material and vegetation of the bioretention basin is presented in Table 2).

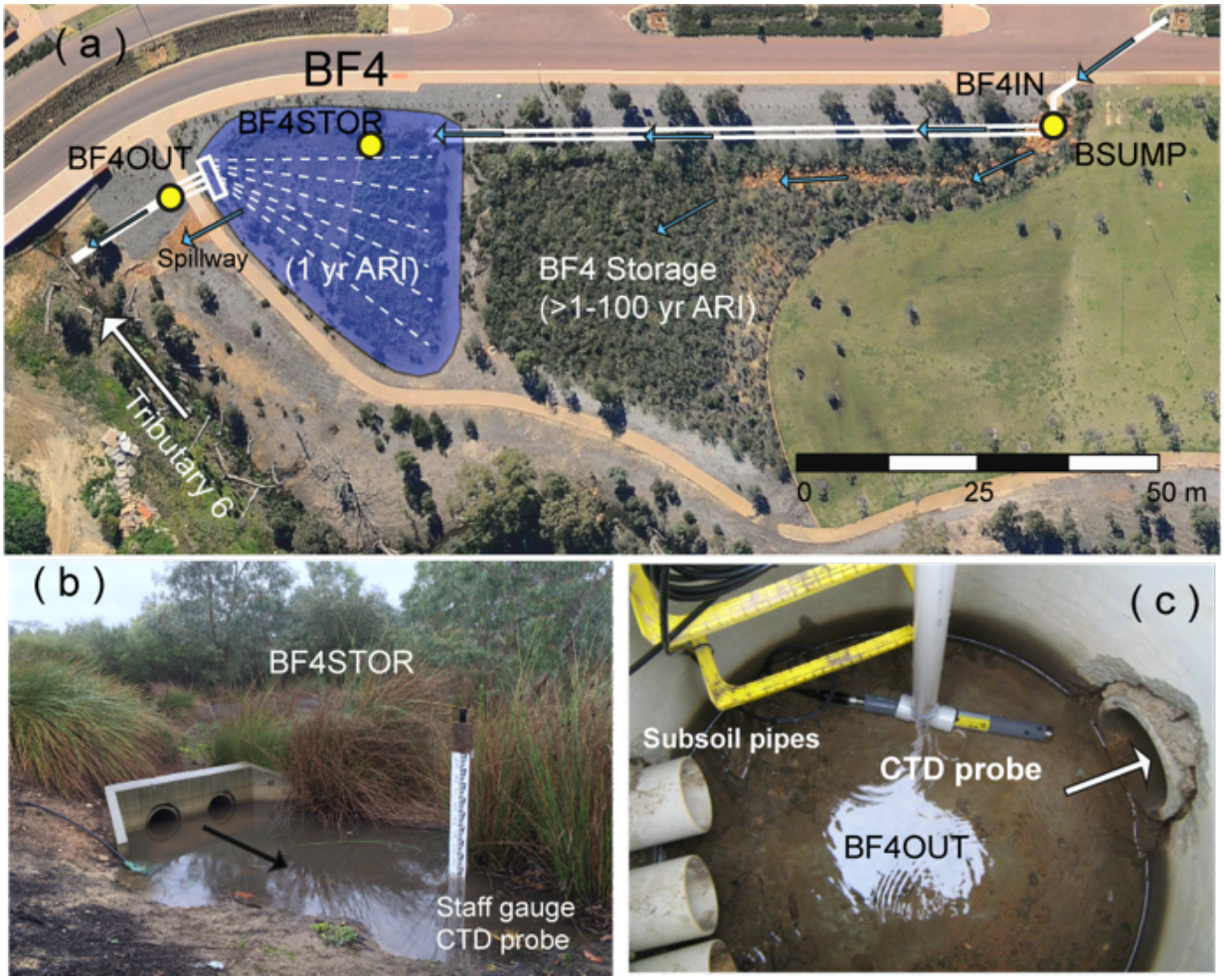

Figure 4: The bioretention basin drainage components and selected monitoring points: a) plan view showing inflow and outflow locations (yellow dots), b) inflow to the basin storage area for treatment, and c) effluent from the filter media flows into the discharge pipe to Cardup Brook Tributary 6. Dashed line in a) indicates subsoil pipes below filter media. Arrows indicate flow direction.

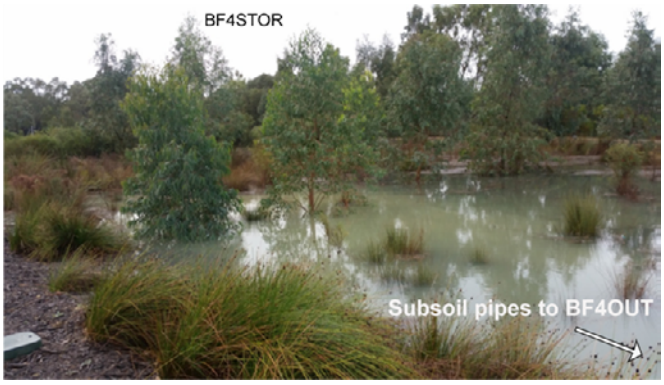

Figure 5: The bioretention basin with standing water.

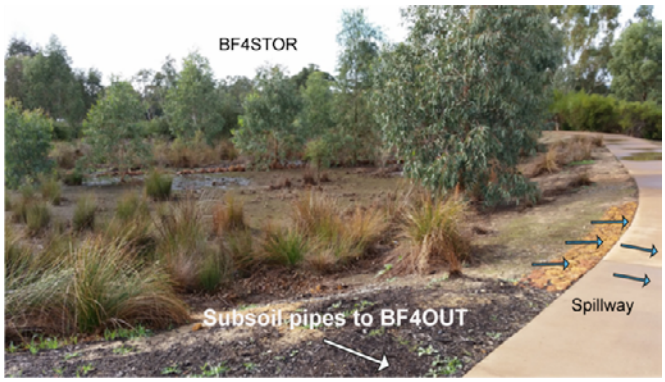

Figure 6: The dry bioretention basin, BF4.

Table 2: Specifications of the bioretention basin (BF4)

Bioretention Basin (BF4)	
Date of construction	2010
Filter media	Red Gingin loam (organic matter 1.16%, pH 6.12, EC 201.8, k 41.6). Minimum 500 mm thick PRI > 5 pH 5.5-7.5 Total clay and silt fraction < 3% in total (w/w) Organic matter content < 5% (w/w) Phosphorus content <100 mg/kg Hydraulic Conductivity (sat) > 6 m/day Light compaction only (JDA, 2009)
Plant species	Baumea juncea, Melaluca lateritia, Juncus pallidus, Ficinia nodosa, Eucalyptus rudis, Melaleuca nesophila, Calothamnus quadrifidus, Callistemon viminalis, Conostylis aculeata
Catchment area and physical parameters	8.7 ha with 27% of impervious area directly connected. Surface slope of impervious areas (roads) ranges from 0.02 to 0.05 m/m. Drainage pipes average density of 164 m/ha and average slope of 0.01 m/m. Subsoil pipes to control groundwater level with a density of 246m/ha.
Dimensions (length, width and depth)	0.35 m deep Surface area of 1200 m^2 Storage capacity of 370 m^3 for 1-year ARI event (36 hr duration used for storage design)
Lining	Lined with clay (natural soil of area)
Outlet mechanism	Slotted pipes (PVC) collect infiltrated water from biofilter media and perched water table. Spillway for overflow to Cardup Brook Tributary 6.

3. Methodology

3.1 Monitoring program

Table 3 presents an overview of the complete monitoring program, and Figure 1, Figure 3 and Figure 4 show monitoring site locations. A description of the sampling methodology is provided in the following sections.

3.2 Hydrological monitoring

Continuous hydrological monitoring stations were installed at five surface water sites (Figure 1). The monitoring undertaken at each station is outlined in Table 3 and photographs of the monitoring setup can be seen in Figure 3 and Figure 4. Theoretical rating equations were developed for each station based on hydraulic conditions and the geometry of pits and pipes. Opportunistic volumetric discharge measurements along the pipe network (stopwatch and flexible buckets) were used to verify and adjust the theoretical rating. The task was possible at BF1 and BF2 outflows (Figure 7) for low flow and at BF4 outflow station for low, mid and high flow conditions. This data was then used to compute the inflows and outflows for the biofilters for each rainfall event, and also to estimate groundwater interaction. Groundwater showed a distinct EC signature and thus the continuous EC readings were used to identify groundwater inflows.

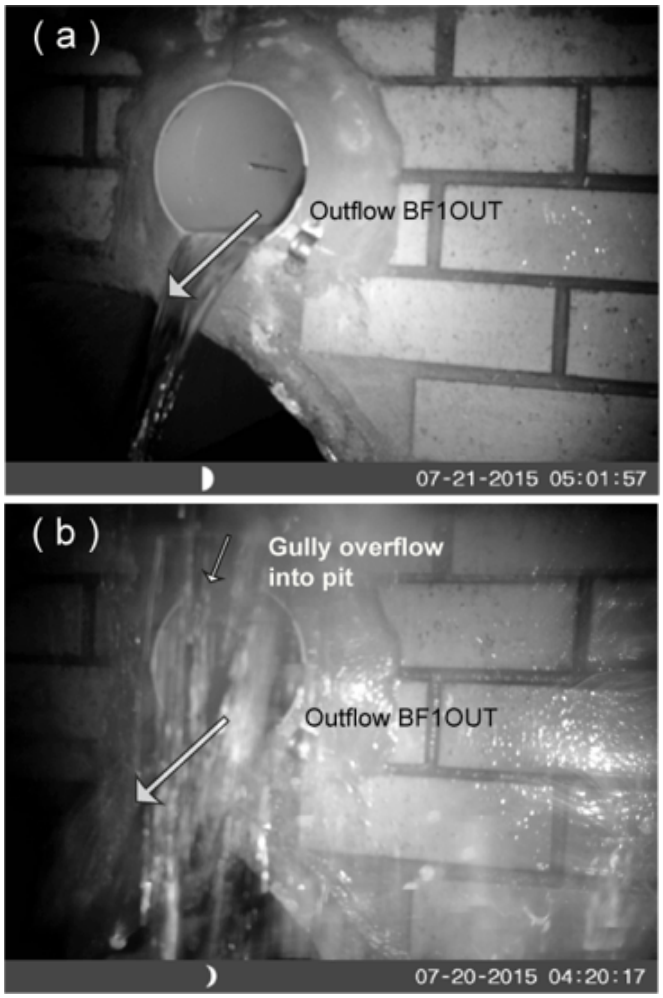

Figure 7: Camera still used in flow monitoring at the Raingardens 1 and 2 outlet stations: a) shows normal outflow, and b) shows additional outflow surface runoff where stormwater has bypassed infiltration and enters from gully overflow. Arrows indicate flow direction.

Table 3: Summary of monitoring program

Component	Parameters	Frequency	Sites
Water Quality	Total nitrogen (TN),	Event based sampling	BF1IN, BF1OUT,BF1, BF2IN, BF2OUT,BF2, BF4IN, BF4OUT, BF4STOR
	Total phosphorus (TP),		
	Nitrate/nitrite (NOx-N)		
	Dissolved organic nitrogen (DOrgN)		
	Ammonium (NH4-N)		
	Filterable reactive phosphorus (FRP),		
	Total suspended solids (TSS)		
	Dissolved oxygen (DO)		
	pH		
	Dissolved organic carbon (DOC)	Sporadic	
	Temperature	Continuous (2-10 minute intervals)	BF1, BF2, BF4IN, BF4OUT, BF4STOR
	Electrical conductivity (EC)		
Hydrology	Water level	Continuous (2-10 minute intervals)	BF1OUT, BF1,BF2OUT,BF2, BF4IN, BF4OUT, BF4STOR
Groundwater			
Water Quality	TN, TP, NOx-N, DOrgN, NH4-N, FRP	Sporadic	BGB1 and BGB2
	Temperature, conductivity, dissolved oxygen, pH		
Hydrology	Water level	Continuous (15 minute intervals)	BGB1 and BGB2
Rainwater			
Hydrology	Total rain (mm)	Continuous (2 minute intervals)	BF4IN

Groundwater bores

Two shallow bores were installed to monitor water level dynamics of the perched seasonal water table. They were strategically installed upstream of the flow gradient (perpendicular) to the main stormwater drainage pipe and local infiltration sources. BGB1 was 35 m upstream, and BGB2 was 225 m upstream (Figure 1). Both locations showed similar sediments in the unsaturated zone: a top layer (to a depth of 0.8 m) with fill material used for the development (sand), a transition to a fine sand until 1 m deep, then finally a sandy clay mottled layer (up to a depth of 3 m). The PVC pipe bores were drilled to a depth of 3 m, with slotted pipe present only in the bottom 2 m to avoid infiltration of rain water. See bore characteristics shown in Table 4.

Perched groundwater sampling was conducted using a low-flow pump after purging the bore. Water quality parameters were measured in the field with a multi-parameter probe (Hydrolab MS5). Water samples for dissolved nutrient analysis were filtered in the field and all samples stored in an esky prior to delivery to the Australian National Measurement Institute (NMI) laboratory in Perth.

Table 4: Shallow bores specifications at The Glades Stage I

	Bore 1	Bore 2
Site name	BGB1	BGB2
Distance from stormwater pipe at Mead Street (m)	35	225
Distance to near subsoil pipe to control GW (m)	7.6	3.8
Depth from top of casing (m)	3.13	3.22
Diameter (cm)	4	4
Slotted length (m)	2	2
Top of casing to ground (cm)	9.35	13.0

Table 5: Description of hydrological monitoring program

Station	Description	Equipment
Raingarden 1 at pit (BF1)	This site received all the runoff generated upstream of this point, including from roads, raingarden outlets (including BF1OUT), subsoil pipes and housing. Water goes to BF2 station (pit) via main drainage pipe at Mead Street.	A CTD (conductivity, temperature and depth) probe (YSI 600 LS) was installed in a PVC well attached to the pit's ladder. The logger was set to 2-minute intervals. A field rugged camera taking pictures at 10-minute intervals was also deployed to identify timing of water sample collection by the autosampler.
Raingarden 2 at pit (BF2)	This site received water from upstream stormwater system, roads, raingarden BF2OUT, BF1 pit stormwater and subsoil drainage pipes. Water goes to BSUMP station via main drainage pipe at Mead Street.	CTD probes (YSI 600 LS and Hydrolab MS5) were installed in a PVC well attached to the pit's ladder. The loggers were set to 2-minute time intervals.
Bubble-up Sump (BSUMP or BF4IN)	This site received all water from Stage 1 A development, including that at station BF2 (pit), and additional runoff from roads and a raingarden effluent and subsoil drainage pipes. Water goes to bioretention basin storage (BF4STOR) for final treatment.	A Unidata water level (pressure sensor) and a tipping bucket rain gauge (RIMCO) were wired to a datalogger with a 3G telemetry (Neon-Unidata) logging data at 2-minute intervals. A CTD probe (YSI 600 LS) was installed and sampled at 5-minute logging intervals. A Solinst logger recording barometric pressure at 5-minute intervals was also located in the recorder cabinet to provide information required for water level corrections of pressure sensors deployed at the site.
Bioretention basin storage (BF4STOR)	This station measured inflow from BF4IN, direct rainfall input, and potential outflow via spillway. It provided water levels for inflow computation, changes in storage and passive tracer for hydrograph separation.	A staff gauge plate (surveyed) and a CTD sensor (Solinst) were installed to collect water levels and electrical conductivity for the surface water storage at 10-minute time intervals.
Bioretention basin outlet (BF4OUT)	This station measured outflow from BF4 via subsoil pipes after treatment. Effluent goes to Cardup Brook Tributary 6.	A CTD probe (YSI 600 LS) was installed in a PVC well attached to the pit's ladder. The logger was set to 2-minute time intervals.
Groundwater bores (BGB1 and BGB2)	These bores measured the perched water table; 35 and 225 m from the main stormwater pipe at Mead Street (see Table 4 for specifications).	Water levels at both locations were continuously monitored at 15-minute intervals using 2 m long capacitance probes (ODYSSEY). Manual water level measurements were taken on 12 occasions to adjust and check automatic data recorded by the water level probes.

3.3 Water release trial

To test if the raingardens would be suitable for performance assessment, a controlled water release trial was conducted on 18 November 2014 at BF1. Specifically, the test aimed to determine:

- Storage volume required to generate outflow from the subsurface pipe.
- Maximum storage capacity to produce gully overflow discharge.
- Exfiltration loss to the surrounding environment.
- Lag time between inflow and outflow.
- Hydrological response to a short water input pulse and flow recession characteristics.

The water release trial was conducted under dry conditions to allow quantification of the maximum water storage at times when water losses such exfiltration and evaporation were high. It also avoided interference with nutrient cycling processes in the subsurface filter media, which was the main focus of the monitoring program undertaken in the winter of 2015.

Two water tankers supplied 60 m^3 of potable water (Figure 8a). A flow bar was constructed to evenly distribute the flow over the central 2 m width of the raingarden, discharging at 4.3 L/s (Figure 8b). At the downstream point, an existing monitoring station (BF2) recorded water level, temperature and specific conductance (electrical conductivity at 25° C) over the duration of the test. A multi-parameter probe logging physical water quality parameters at BF1 was also deployed in order to trace the inflow of fresh water from the water tankers. Water samples were collected over the duration of the test for later water quality and nutrient analyses in the laboratory.

As the filter media reached saturation and outflow via the slotted subsoil pipe occurred, volumetric discharge measurements were taken at regular intervals (~10 minutes) using a container of known volume and a stopwatch.

Inflow started at 4.3 L/s (or 260 L/min from the tanker gauge). After 50 minutes, the outlet began to flow. Inflow discharge was later decreased by approximately 2 L/s to simulate a smooth falling limb of the hydrograph and then rapidly increased to 6.5 L/s to simulate water input from a short duration-single peak rainfall event (see Table 6 for details).

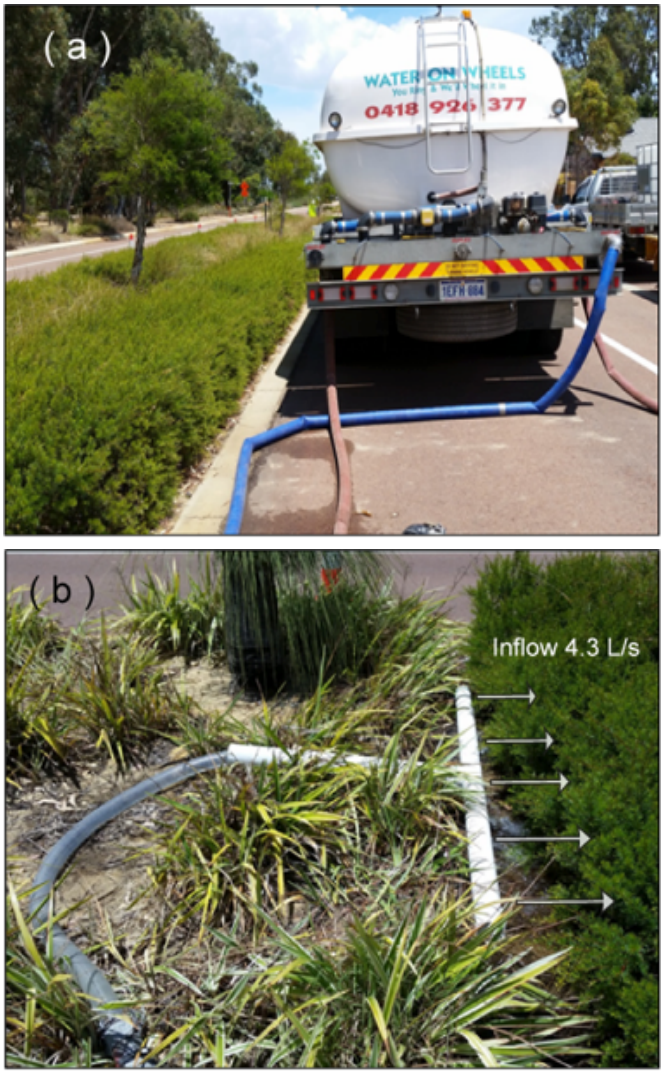

Figure 8: Water dosing trial at the raingarden BF1: a) tanker delivering gauged flow to raingarden, b) water distribution pipe for inflow at the raingarden. Arrows indicate flow direction.

Time	Action
09:10	Trial started at 4.3 L/s
11:50	Flow rate halved to approximately 2 L/s
12:30	Flow rate raised to approximately 1.5 times original flow – 6.5 L/s
13:15	Pumping ceased

Table 6: Pumping details for water release trial.

3.4 Water quality sampling

Due to the variable nature of flow conditions in the raingardens and the bioretention basin, a range of methodologies and equipment was used to collect water samples for nutrient analysis. The sampling strategy (use of surface water traps, two-bottle autosamplers and cameras) also addressed some of the challenges at the site such as the rapid response to rainfall events and shallow depth of flow in the raingarden, timing of the occurrence of the events (often at midnight and early morning), budget constraints, short term monitoring program (1 year) and vandalism. All sampling points were in public open space with limited space for large equipment housing structures.

Water quality monitoring and water sample collection were conducted by research teams from Department of Water of Western Australia (DoW) and UWA-CRCWSC to maximise sampling coverage across the runoff events. In situ measurements of temperature, specific conductance, pH and dissolved oxygen were taken using multi-parameter probes (YSI Pro Plus and Hydrolab MS5). Water samples for dissolved nutrient analysis were filtered in the field (0.45 µm), and all samples were stored on ice and transported to NMI in Perth, complying with DoW Chain of Custody processes.

Raingarden (BF1)

At BF1 inflow (BF1IN), water sampling was done using surface water runoff traps (Figure 9). Three of these were placed at even spacing along the raingarden length. The traps consisted of a shallow well with a mesh covering slots in the upper portion of the pipe allowing surface flow to enter, and a lid to seal the sample (Figure 9a). The traps collected water for events capable of developing surface runoff with sufficient depth to reach the opening; this was estimated during the field trial to be at flow discharge rates of 4 L/s. Sampling represented high flow rates as we expect water to infiltrate into the media under low flow rates. Samples were collected within a few hours after an event using a small diameter plastic bailer.

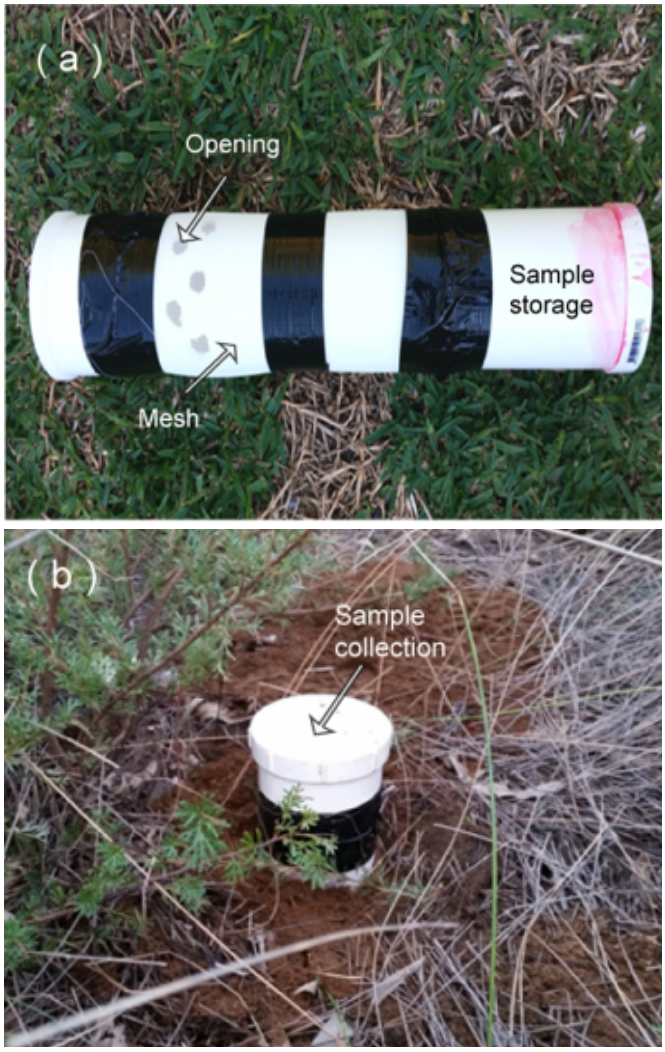

Figure 9: Water sample collection at BF1 inflow: a) surface flow trap used to collect sheet flow into the raingardens with view of opening with mesh to capture surface runoff, b) field deployment.

The BF1 outflow (BF1OUT, via its subsoil pipe) was sampled using an automatic sampler (Model WS750, Global Water Inc.) inside a rugged case and attached to the pit ladder. This sampler had two peristaltic pumps that could be independently triggered, two 4 L containers for water samples, a water sensor to trigger the sampler and two intake hoses. Figure 10a shows the trigger and hose setup inserted into the outflow subsoil pipe.

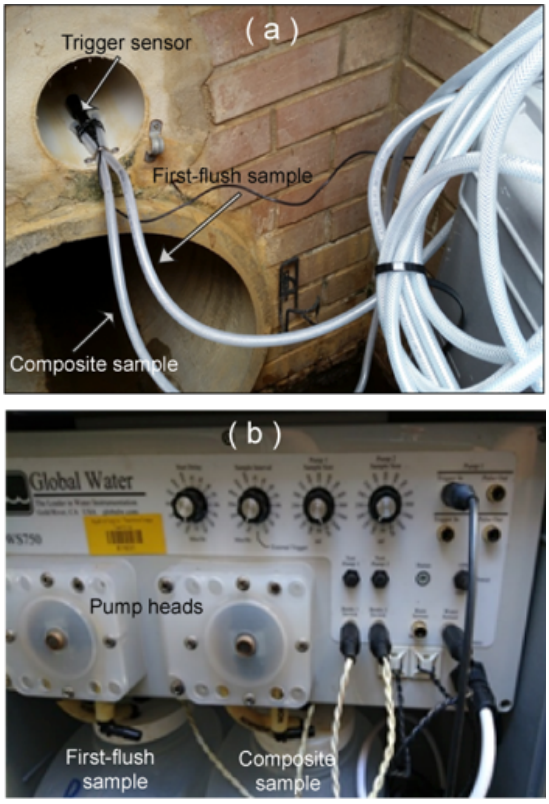

Figure 10: Automatic water sampler at BF1 outflow: a) sample trigger and two intake hoses, b) peristaltic pump control panel and bottles.

The first bottle was triggered to fill as soon as flow commenced and thus captured the "first flush". The second bottle collected a composite sample made up of 100 mL collected every five minutes, to cover a 3 hour 10 minute period until the bottle was filled (Figure 10b). The composite sample bottle could also collect multiple events if the first event finished and the bottle was only partially filled. This autosampler setting allowed sampling over more than 75% of the duration of the outflow hydrograph for small and minor events and 60% for major events (measured at approximately 5 hrs). Additional manual grab samples were also collected if the outflow was active during field visits.

Bioretention basin (BF4)

The configuration of the pit was controlled by its hydraulic functioning, and this configuration together with public access issues made implementation of an automatic sampling system difficult at the BF4IN inflow station (Figure 4a). Consequently, manual grab samples were collected to characterise water inflow to the bioretention basin. Grab samples were collected prior to, during and after a flow event; the timing of sampling was informed by Australian Bureau of Meteorology forecasts and telemetry data (water level at BSUMP) that indicated high flow conditions. Finally, 1-2 grab samples were collected within 12 hours after the event, ensuring we captured the recession period of the hydrograph. This task was coordinated between the DoW and UWA research teams.

An automatic water sampler similar to the one described for BF1 outflow above (Model WS201, Global Water Inc.) was used to sample the bioretention basin outflow (BF4OUT) (Figure 11). The first bottle collected 4 L of the "first flush" runoff out of the bioretention basin filter media while the second bottle collected a composite sample (150 mL every 30 minutes to 1.5 hours depending on the season) over the duration of the event. This autosampler setting allowed sampling for outflow durations of 14 - 36 hr, which was compatible with outflow hydrographs resulting from minor and major events respectively (see Figure 26 and Figure 40 in Appendix 1-B).

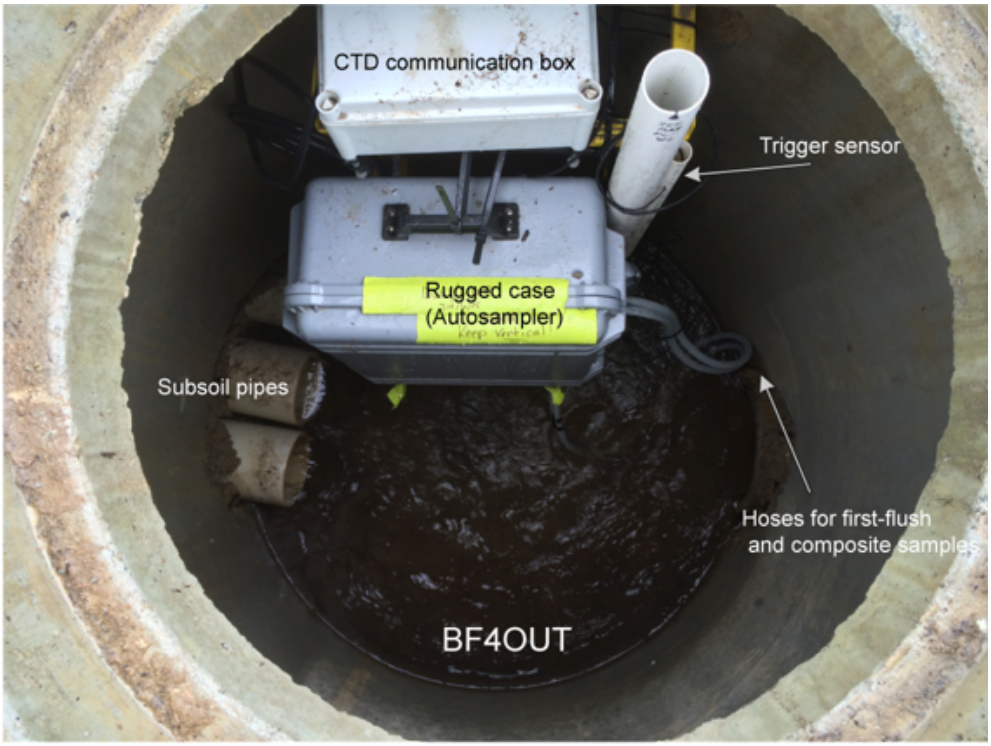

Figure 11: Water sampler collection system implemented for the bioretention basin outflow (BF4OUT).

Manual grab samples were also collected during baseflow conditions. Figure 12 shows the temporal coverage of the sample collection at this station compared with water levels at the outflow. The sampler trigger was initially located at an elevation corresponding to the invert of the outflow pipe but was raised during August-September as baseflow conditions were established inside the pit (see water level in Figure 12).

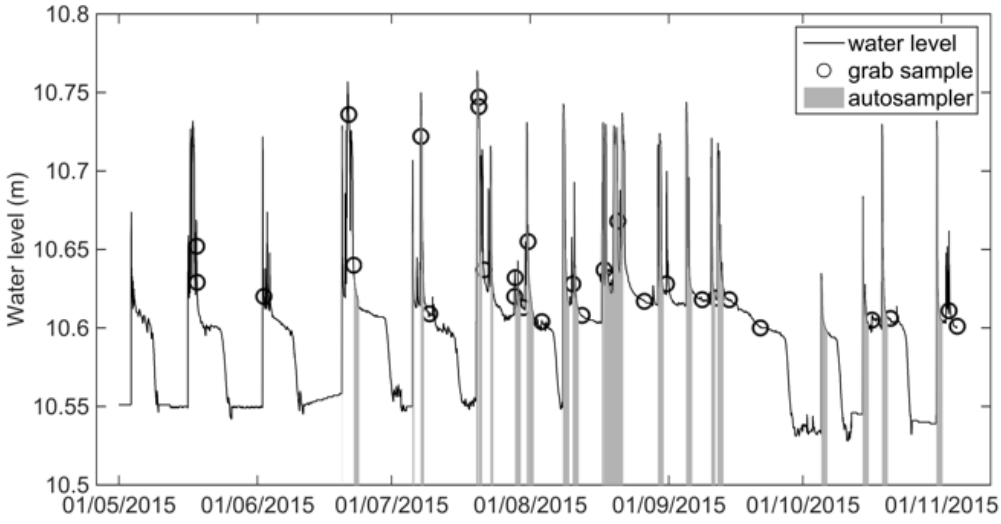

Figure 12: Water sample collection strategy implemented at bioretention basin outflow (BF4OUT) during 2015.

3.5 Efficiency calculation methods

The event mean concentration (EMC), defined as the total nutrient load (mass) divided by the total runoff volume of an event, has been recommended by guidelines to assess nutrient removal efficiency by structural elements such as biofilters (Winer, 2000; DoW, 2004). EMC values for the inflow and outflow are used to evaluate the percentage of nutrient removal as:

$$\text{EMC attenuation } (\%) = \left(\frac{EMC_{in} - EMC_{out}}{ECM_{in}} \right) \times 100 \quad (1)$$

where EMC_{in} is the nutrient (total or species) mean event concentration at the inflow and EMCout is the nutrient (total or species) mean event concentration at the outflow.

As described in Section 3.4, limitations in the water sample collection at inflow (few manual grab samples per event) and outflow (automatic time-weighted composites) stations made it difficult to use Equation 1 for efficiency calculations. Estimation of EMC requires temporal resolution of nutrient concentration over the course of an event, by either sequential sampling techniques (a minimum of five water samples by automatic or manual collection) or flow-weighted composite samples (collected by an automatic water sampler triggered by flow sensors).

In the present work, the change in nutrient (nitrogen and phosphorus) mass from inflow to outflow was used to assess nutrient removal efficiency. The percentage removal or load attenuation was used as a measure of nutrient removal efficiency as:

$$\text{Load attenuation } (\%) = \left(\frac{L_{in} - L_{out}}{L_{in}} \right) \times 100 \quad (2)$$

where L_{in} is the nutrient load at the inflow, calculated as the product of the inflow arithmetic mean concentration of available samples and the inflow volume, and L_{out} is the nutrient load at the outflow, calculated as the product of the outflow concentration of the time-weighted composite sample and the outflow volume. Note that inflows and outflows may include shallow water table contributions if the system interacts with groundwater.

For each rainfall event, the arithmetic mean concentration at the inflow (hereafter referred to as the mean) was estimated using available nutrient concentrations. We used the average nutrient concentration in grab samples of surface runoff flowing along the raingarden at BF1 (three samples), and the average nutrient concentration in grab samples collected prior to, during, and after the event at the bioretention basin BF4 (two to four samples). For the raingarden and the bioretention basin outflows, we used the nutrient concentration in the time-weighted composite sample collected by the autosamplers.

Each rainfall event was defined and then loads were calculated by multiplying the total volume of event water at the inflow (or outflow) by the corresponding arithmetic mean nutrient concentrations. Load attenuation (%) value was calculated using equation (2).

We tested whether the nutrient concentrations of the time-weighted composite sample could indeed be considered representative of EMC at the outflow station. We used a linear interpolation of concentration values obtained at different flow discharges over the duration of the event: first-flush during the rising limb, time-weighted composite sample over the event and manual grab samples during the recession limb of the hydrograph. Linear regression between EMC and composite sample concentrations for TN, TP and dissolved species showed R^2 values > 0.9 for small and minor events. The R^2 values dropped to 0.85 when considering major events for TN and TP but not for dissolved species. These results are promising for practical applications but more investigation is needed due to the site specific nature of the findings.

Finally, nutrient concentrations were also compared to concentration trigger values for the protection of estuaries in south-west Western Australia (ANZECC & ARMCANZ, 2000). These were deemed the most relevant for this case because Cardup Book discharges to the Serpentine River that flows into the Peel-Harvey Estuary; the Estuary is subject to severe water quality problems (EPA, 2008).

4. Water balance analysis

4.1 Rainfall and groundwater

The mean annual rainfall for the area is approximately 859 mm (BOM, 2015). However, our BSUMP rain gauge only recorded 611.8 mm, which is 247 mm below the long-term average. The observations from BSUMP were of similar magnitude and monthly distribution to that of the nearby BOM station (634.9 mm at Anketell).

The shallow water table developed late in the winter season and its dynamics varied depending on location within the urban development (Figure 13).

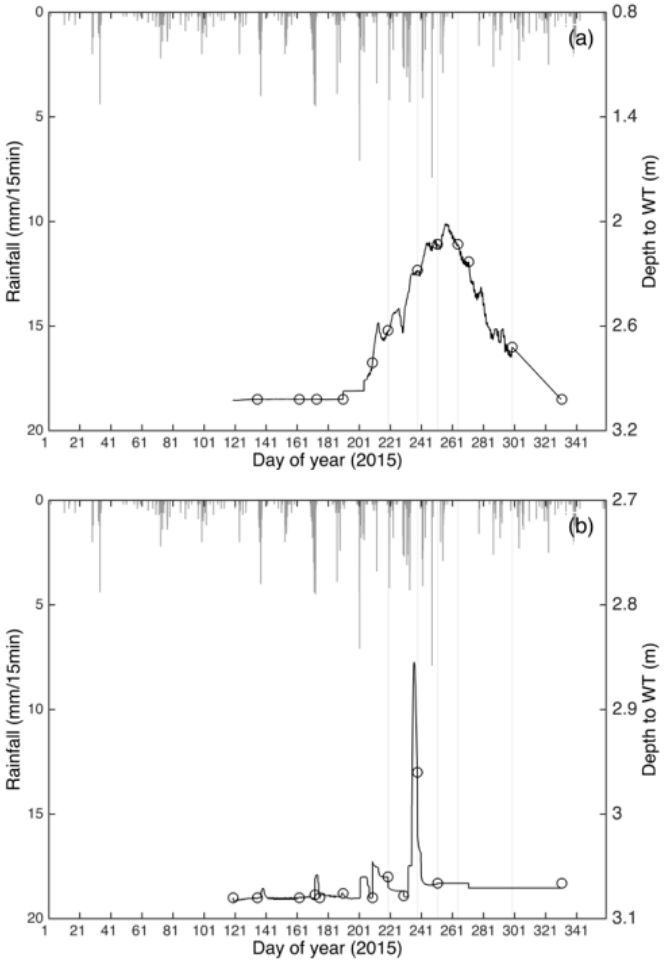

Figure 13: Time series of rainfall and water table depth at The Glades Stage 1: a) BGB1 and b) BGB2. Data corresponds to 15-minute intervals. Depth to water table (WT) is referenced to ground level. Symbols represent manual water level readings.

Water table levels at BGB2, located 225 m upstream of the drainage pipe at Mead Street, only responded to four rainfall periods. The major rainfall event in August (from day 230 to 241 in Figure 13b) generated saturated conditions for a period of two weeks. No response to rainfall was recorded at this location towards the end of the monitoring period. It is likely that the observed hydrological response at BGB2 was the result of combined topographic control (high elevation in the urban development) and the presence of subsoil pipes to control groundwater (see Table 4).

At BGB1 (35 m upstream of the drainage pipe at Mead Street), no water table changes were recorded until early July (day 181 in Figure 13a), despite minor and major rainfall events in mid-May (33.4 mm) and mid-June (61.2 mm). The first noticeable increase in the water table was observed on 9 July after two minor rainfall events (totaling 28.8 mm), followed by 71.8 mm of rainfall for the second half of July. The water table level continued to rise during August and reached a maximum level of 2.01 m on 13 September (day 256 in Figure 13a). Finally water levels began to recede, as the temperatures increased and evaporative demands appeared to outweigh rainfall inputs by small events. The bore dried out by end of November 2015.

Based on the topography of the area and the elevation of different elements of the drainage network at Mead Street (main stormwater drainage pipe and pits), it was possible to determine the interception of the shallow water table with the stormwater system. There was no direct interaction with the raingardens outflow pipes, however, the water table was well above (by 0.5 m) the invert of the stormwater pits at Mead Street and was effectively contributing to the flow of the main drainage network and intercepting the bioretention basin subsoil outflow pipes.

4.2 Raingarden hydrology

The inflow and outflow hydrographs for the field trial are presented in Figure 14. At a flow rate of 4.3 L/s, it took 50 minutes for infiltrated water to begin discharging from the outflow. The outflow hydrograph showed a lag in response to the second peak and two clear recession periods as water drained from the media.

Using the volumetric data derived from this trial it was possible to quantify key parameters needed to describe the hydrological functioning of the raingarden. Namely, a threshold volume of 13.25 m^3 was required to initiate outflow, and 19.1 m^3 to wet up the entire length of the raingarden. Further, a total volume of 31 m^3 was required to generate surface gully overflow.

The dosing trial showed that the raingarden worked as designed. Of the 60 m^3 pumped into the raingarden, approximately half flowed through the media and reached the outlet pipes, 5 m^3 was exfiltration to surrounding earth, and 25 m^3 was available for plant uptake, evapotranspiration, and longer term biological processing. The saturated hydraulic conductivity of the filter media as demonstrated by the dosing trial was high and was able to handle a flow rate of up to 5 L/s.

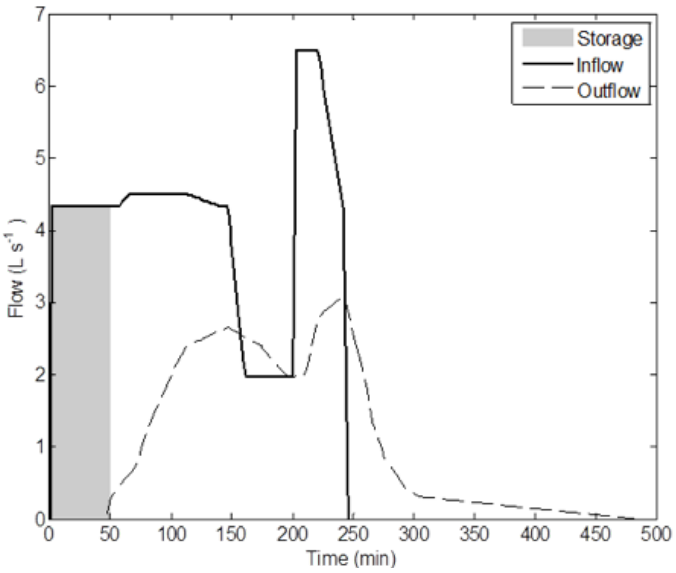

Figure 14: Inflow and outflow hydrographs recorded over the field trial test.

4.3 Inflow modelling

The rainfall data, collected at 2-minute intervals, was used to model inflow into the raingardens. The physical parameters of the raingarden catchment were obtained from survey data (JDA, 2009) and digitised Nearmap photo images (April 2015) using mapping software packages. These are shown in Table 7. A numerical code based on the kinematic wave theory (Lighthill and Whitman, 1955; Dawdy et al., 1978) was used to simulate rainfall-runoff transformation and routing of the storm flow. Effective rainfall was computed after taking the initial abstraction using the SCS Curve-Number method (USDA, 1986) from the 2-minute rainfall data input. In the model, flow routing takes place as overland flow (OVF) discharging into shallow depth concentrated streams that conveyed runoff to the raingarden. This was verified and modified based on the results from the water release trial. The dynamic flow routing was done by a fully mass-conservative explicit numerical scheme (Li et al., 1975) and it provided storm flow hydrographs at a sub-metre spatial scale at every 2-minute time interval.

Since the numerical scheme used by the kinematic wave model preserved water mass, model performance was tested against instantaneous peak flow discharge obtained from the rational method. In line with the Stormwater Management Manual WA (DoW, 2004, p 99), for a time of concentration value of 10 minute used in the design of the flow capacity of raingardens, a 34 mm/h rainfall intensity (1 year ARI) results in a peak flow discharge of 16 L/s. This value is consistent with the recorded event on 19 July, 2015 that generated a peak flow value of 17.8 L/s for a rainfall intensity of 37 mm/h over a 10-minute period.

Table 7: Catchment physical parameters contributing to raingardens BF1 and BF2 used for rainfall-runoff transformation. Slope and OVF parameters correspond to mean values of modelling elements.

	BF1	BF2
Catchment Area (ha)	0.209	0.215
Slope (m/m)	0.0309	0.0263
Flow length (m)	22.9	24
OVF roughness	0.1	0.1
OVF area (m^2)	240	214
Modelling elements (OVF)	15	15

4.4 Outflow modelling

Catchment area and slope were almost identical (Table 7) and numerical modelling for rainfall-runoff demonstrated similar inflow hydrological responses for both raingardens. Therefore, due to physical constraints of the system (interference of flow conditions by autosampler trigger and hoses at BF1OUT) resulting in more accurate data from BF2OUT, this data was used to calculate outflow discharge for the raingardens. To support this, still pictures taken at the outflow of BF1OUT and BF2OUT (Figure 7) were loaded into a photo editing software and scaled to extract information on flow width and depth, time stamp and discharge conditions during rainfall events. Flow discharge was computed using Manning's equation and critical depth formula for a circular pipe for comparison. Estimated flow rates were cross-checked with volumetric discharge measurements obtained during field visits (four) and those undertaken during the water release trial.

A total of 18 outflow events between July and December 2015 from the raingarden subsurface pipe were documented. This represented 53% of the total number of events capable of generating runoff in 2015. A total of 34 inflow hydrographs corresponding to rainfall event magnitudes from 2.6 mm to 40.8 mm were generated for water balance and nutrient load computations for the raingardens. Modelled inflow and measured outflow hydrographs are presented in Appendix 1A.

Raingarden outflow hydrographs for ungauged events (some of which have available nutrient data) were obtained from a simple water balance model following Burns et al. (2015) at 2-minute intervals using parameter values calibrated for the field trial and monitored events over the winter season. The water balance model outputs reproduced outflow hydrographs reasonably well with a difference of 3% for the total event volume and a response that was ahead of the observed hydrograph. Figure 15 shows an example of the model output corresponding to a major event (43.6 mm) on 19 July and 20 July (see also Figure 28 in Appendix 1A). The model was tested against the 18 measured outflow hydrographs before its use in predicting outflow hydrographs for ungauged events.

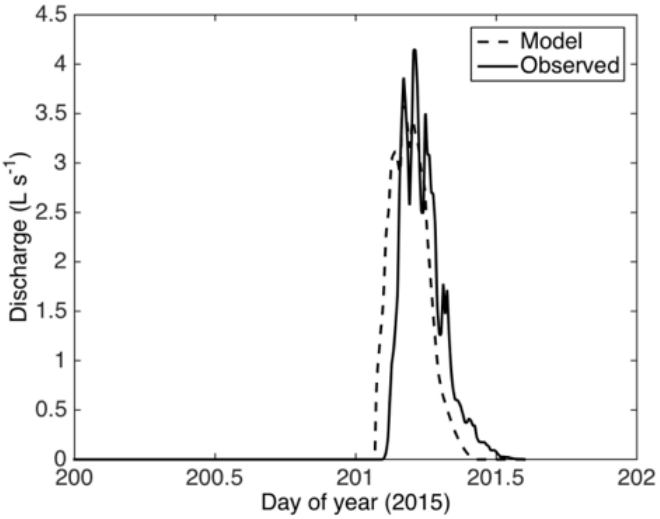

Figure 15: Observed and simulated raingarden outflow hydrographs for a single event.

Figure 16 presents the water balance for the 34 rainfall events generating runoff into the raingarden in 2015. The effect of rainfall characteristic (intensity, amount and duration) and seasonality were more important factors than antecedent moisture condition prior to a rainfall event, in generating outflow from the raingarden via the subsurface pipe.

From January to June in 2015, rainfall events generating more

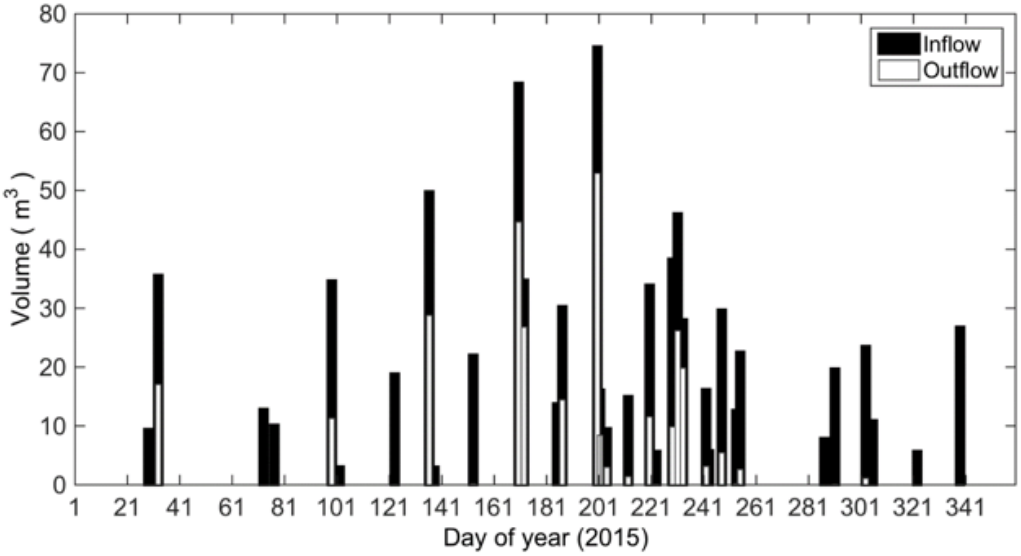

Figure 16: Inflow and outflow volumes at the raingarden for all rainfall events in 2015 against day of year from 1 January 2015. Note that the bar height represents total volume for both the inflow and the outflow.

than 30 m^3 of total runoff resulted in outflow hydrographs. With the exception of one small outflow on day 301 (high intensity-short duration event) no outflow runoff was generated from events occurring in the late spring and early summer season.

Most of the outflow runoff was generated over the August-October period when events of less than 30 m^3 in volume were capable of generating outflow runoff. The change in the water balance could not be explained by antecedent moisture condition prior to the occurrence of individual rainfall events, but were likely due to some hydrological change experienced by the area. Volumetric ratios (VR = Volout/Volin) were between 65 to 77% for rainfall events exceeding 40 mm. In general, events of less than 20 mm resulted in a VR from 26 to 48% with the later corresponding to a high intensity event (imax_10 = 31 mm/h) on 1 February. A VR of 20% was obtained for an isolated event of 17.8 mm (imax_10 = 42 mm/h), which is close to the 1 year ARI-1 hour event. All events recorded after day 251 (10 September) had rainfall amounts of less than 20 mm and VR values from 0.2 to 12%.

Results from the water balance model for all rainfall events indicated that the total inflow to the raingarden was partitioned as follows: 37% as subsurface outflow runoff, 38% local recharge (leakage) and 25% as soil moisture available for the vegetation and evaporative losses. A summary of the values can be found in Table 16 in Appendix 1A.

It is interesting to note that the volumetric ratios for events of less than 20 mm of rain were higher than the design value (~ 30% for ARI 1 year event) over the period August-September. At this time the water table was well above the invert of all stormwater pits at Mead Street and closer to the raingardens outflow pipes, intercepted the basin and altered the hydrological dynamics of the system.

4.5 Bioretention basin hydrology

A total of 36 rainfall events were analyzed to calculate inflows and outflows to the bioretention basin (Figure 17). Eight events required adjustment of water levels at the inflow station BSUMP due to backwater effects from the surface storage area. Corrected water levels were then used to compute inflow discharge by means of the rating table for the station (DoW WIR-Hydrosmart). Measured inflow and outflow hydrographs for selected events are presented in Appendix 1B .

In general, outflows and consequently VR were highly dependent on two factors: the ponding area effectively contributing to infiltration and antecedent sub-surface conditions at a seasonal scale. The first factor is a function of the inflow volume, which determines the ponding area of the basin that is effectively contributing to the bioretention outflows infiltration and ultimately the subsurface outflow (via the pipes). The second factor reflected important changes in the underlying hydrology of the area and was highlighted early in the wet season by frequent small rainfall events (< 10 mm) with an average VR of 20.5%. Between June and September VR increased to 63.2%; from October to November it decreased again to 20.6%. A similar seasonal pattern for VR was observed for minor and major events in the 20-30 mm range as average values increased from 48% to 80% over the same periods. As expected, major events (> 40 mm) always showed high VR (on average of 93%).

As was found in the raingardens, high VR over the winter period may reflect an important shift in the subsurface hydrology of the area with increasing interaction with the shallow water table. For the purpose of the present report, no attempt has been made to undertake a detailed water balance for the bioretention basin to address the proportion of missing water and its pathways such as deep infiltration and leakage into the shallow water table and water storage (as soil moisture) in the subsurface biofilter media (estimated to be at 25 m^3 at field capacity moisture condition) for evaporative losses. However, a preliminary model exercise conducted by Sidoti (2015) indicated the likelihood of a shallow water table contribution of 20% of the total outflow volume from late July to the end of August. This has implications for bioretention function and assessment of effectiveness, when interpreting data for nutrient attenuation.

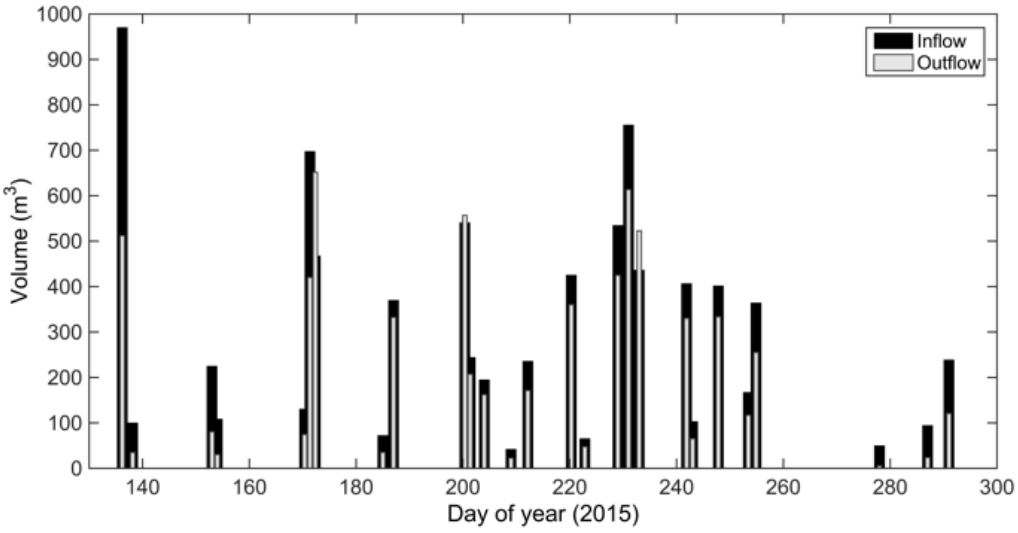

Figure 17: Inflow and outflow volumes for the bioretention basin BF4. Time period corresponds to May-November 2015. Note that the bar height represents total volume for both the inflow and the outflow.

4.6 Groundwater interactions

The water balance modelling of the raingarden, comparisons to water table levels, as well as construction specifications (JDA, 2009), showed that the shallow water table did not directly interact with the raingardens. Shallow saturated flow in the filter media (throughflow) was intercepted by subsurface drainage and entered the piped system below the raingardens.

However, hydrometric data at bioretention basin outflow BF4 indicated that continuous baseflow discharge was established from mid-August to late-September (see water levels in Figure 12), so further analysis was warranted.

A chemical hydrograph separation (CHS) technique was used to identify two water pathways and volumetric contribution towards BF4 outflow: a) Inflow/surface storage water passing through the filter media and b) shallow water table discharge intercepted by subsoil pipes. Specific conductance (SC; EC at 25°C) was used as the passive tracer in a two-component mixing model (Sklash and Farvolden, 1979). This was feasible because of large differences in SC values between water sources and its suitability as a tracer in urban catchments (Pellerin et al., 2008).

Time series of SC data and event hydrographs for BF4 outflow (at 2-minute time intervals) were used for the mixing model. Observed SC values prior to each rainfall event characterised either water stored (residual saturation degree) at the bottom of the filter media surrounding the drainage pipes (when WT is not present) or WT contribution as intercepted by the subsoil drainage (when WT is present).

Timing for WT contribution was identified from hydrometric data for BF4 outflow (Figure 12), water table levels (see Figure 13) in the shallow bores and a remarkable increase in SC values for BF4 outflow (range 600-1000 µS cm^{-1}) exceeding those corresponding to subsoil media of the raingardens at The Glades (SC range 180 - 360 µS cm^{-1}). For events less than 20 mm, SC of the inflow was used as a time-varying tracer value; for events larger than 20 mm, SC of the surface water storage water (at 2-minute time intervals) was used as a tracer representative of water entering the bioretention basin.

Figure 18 shows results of CHS for two events, without and with water table contribution.

The results indicated that during early events in the season between January and July (7 mm to 40 mm), residual saturation (water held at the bottom of the bioretention basin filter media) contributed 21% (± 6%) on average towards the BF4 total event flow (no perched groundwater developed at this stage). As the perched groundwater develops, its contribution towards the BF4 outlet was quantified on average at 18% (± 7.7%).

Although the differences in the proportion of groundwater contributing towards the BF4 outflow appeared not to be significant with and without the water table influence, there is a significant difference in the "average volumetric contribution" value over the course of the events, estimated at 20 m^3 and 49 m^3 with and without water table influence respectively.

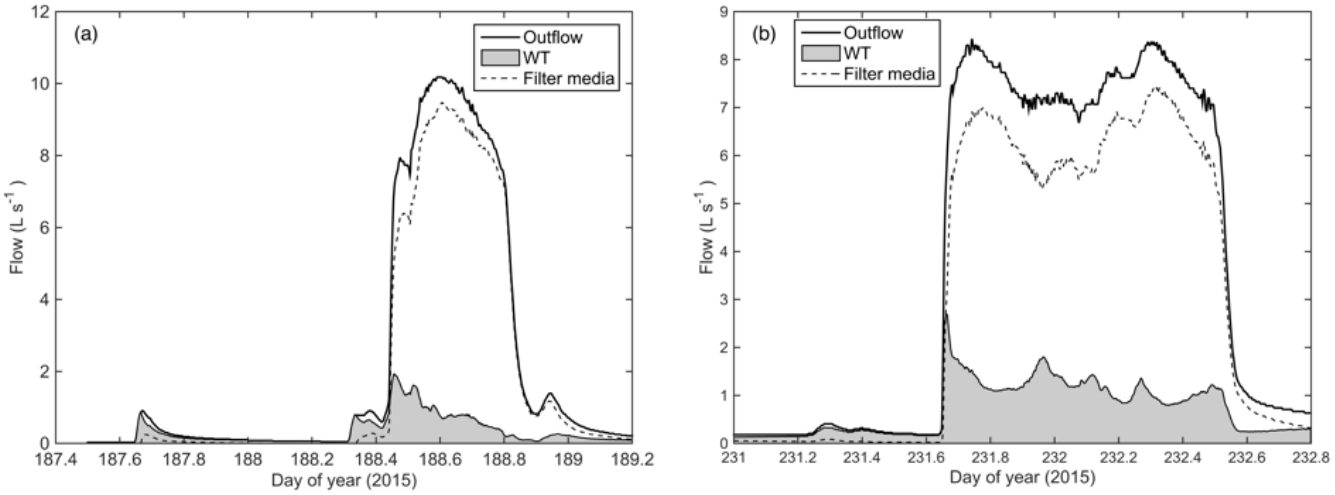

Figure 18: Results of chemical hydrograph separation for two events: a) without and b) with water table contribution. Shaded area in a) represents water holds in the subsoil media and in b) represents water table contribution.

5. Hydrological performance

5.1 Raingarden

The hydrological performance of the raingarden for at-source control in terms of volume and peak flow reduction was excellent (see Table 8). The raingarden achieved an average event volume retention of 68%, with a variable range from 24-99% depending on storm size and antecedent conditions. Volumetric control by the raingarden under wet conditions for major events was 29% on average and similar to the average value reported in the literature (Hatt et al., 2009). Note that this hydrological performance was calculated for storms that have matching water quality data. A detailed water balance, that includes all inflows and outflows, irrespective of whether water quality data is available, is provided in Table 16 in Appendices 1A.

The reduction in peak flow was 89% across the season and a minimum of 80%. This is larger than those reported in the literature at 80% (Hatt et al., 2009; Payne et al., 2015).

The good performance in both volumetric control and peak flow reduction was largely due to the physical dimensions (40 m x 4.5 m), which are proportioned appropriately for the catchment size, and the appropriate selection of filter media which was able to retain volume and allow infiltration to surrounding soils (estimated at 38% of the annual water input) as well as evapotranspiration.

Small runoff events are completely absorbed by the raingarden, which required a minimum of a 10 mm event to generate flow at the outlet. Therefore, these raingardens help protect the receiving aquatic ecosystems from frequent flashy flows that could degrade them.

Table 8: Hydrologic performance of the raingarden (BF1) for events with corresponding water quality data.

Event	Inflow [L]	Outflow [L]	Retention [%]	Peak Inflow [L/s]	Peak Outflow [L/s]	Peak Flow Reduction [%]
17/5/15	37758	28832	24	14.7	2.1	86
19/6/15	84775	43813	48	15.2	3.1	80
20/7/15	83333	51658	38	22.7	4.1	82
31/7/15	13349	1416	89	8.8	0.5	95
17/8/15	27992	2424	91	11.0	0.7	93
19/8/15	21461	3326	85	7.7	0.8	90
20/8/15	27841	12045	57	9.7	1.3	87
30/8/15	20162	3051	85	10.0	0.6	94
10/9/15	15772	182	99	3.1	0.1	98

5.2 Bioretention basin

Rainfall event characteristics were considered in assessing hydrologic efficiency and nutrient attenuation performance. One rainfall event on 4 September 2015 had similar characteristics of the 1 year-ARI (Imax_10= 42 mm/h, total rainfall 17.8 mm) while most of the events fell within the most frequent events for treatment purposes (6-month ARI). Minor and major rainfall events (→15 mm each) are be also reported together to indicate performance of the system under overload conditions. Table 9 summarises the hydrologic efficiency of the bioretention basin over a range of events.

Firstly, a reduction in volume of approximately 16% was achieved for rainfall events close to design conditions (see events on 8 August and 4 September in Table 9). Water levels at the surface storage reached 0.3 m and 0.33 m for a short period during the first and second events respectively. Lack of volume reduction may reflect the high water table level in the area at the time of the event reduced water losses from the system (reduced infiltration); this result could also be attributed to additional contribution from the water table to the outflow.

Four small events (5-14 mm) displayed some degree of dependency on seasonality and achieved the design volumetric reduction. Two events in the wet winter season showed 28% volume reduction, slightly increased to 30% by September and reached 50% by October. These values were significantly larger than expected and likely reflect the increase in water losses via infiltration and evaporative demands; WT levels were rapidly dropping below subsoil pipes by October.

Major rainfall events occurred from May to August 2015 as the result of particular weather systems affecting the area over a 48-72 hour period, with cumulative rainfall amounts varying between 45 to 70 mm. Such events comprised a succession of 20 mm events and were responsible for the large mobilization and redistribution of nutrients within the catchment and contributed to the acceleration of shallow water table development.

For these major events, there were no significant reductions of the outflow volume (from 5% up to 8%) with the exception of one event under dry antecedent condition, which reached a volume reduction of 20%. Over the course of these events, water levels in storage (the basin) ranged from 0.44 m to 0.51 m and rapidly dropped over a 15-minute time period. These water levels were above the overflow level set for the storage and can account for the small volume difference unaccounted at the outflow.

The bioretention basin achieved its intended hydrologic performance in relation to peak flow control with peak flow reduction between 61 % and 95 % across events of different magnitude and season. Table 9 presents the summary for selected events.

Table 9: Hydrologic performance of the bioretention basin (BF4).

Event	Inflow [L]	Outflow [L]	Retention [%]	Peak Inflow [L/s]	Peak Outflow [L/s]	Peak Flow Reduction [%]
21/06/15	1166424	1071508	8	53.35	10.59	80
6/07/15	370491	332293	10	38.96	10.17	74
20/07/15	244773	206990	15	27.76	6.77	76
31/07/15	236370	171200	28	30.48	8.62	72
8/08/15	425907	360057	15	48.61	9.63	80
10/08/15	65840	47348	28	15.14	4.48	70
17/08/15	535227	424808	21	47.62	8.61	82
19/08/15	1193070	1136125	5	61.6	9.12	85
4/09/15	402166	333474	17	188	9.73	95
11/09/15	364788	254822	30	18.67	7.3	61
18/10/15	239255	120522	50	33.85	8.54	75

6. Nutrient removal nefficiency

6.1 Groundwater nutrients

The preliminary nutrient concentration data for the water table is presented in Figure 19. Specific conductance (electrical conductivity at 25°C) values showed small variability across the season with a mean value of 1556 µS cm^{-1} (± 32 µS cm^{-1}) and the highest value coinciding with the time of the water table peak around mid-September. However, both TN and TP concentrations showed a contrasting pattern to that of specific conductance, with higher concentrations found towards the end of the wet season. This seems to be the result of infiltration of rainfall characterised by low nutrient levels that initially caused the decline in concentrations of TN and TP (early August 2015).

Later, the rising water table level resulted in an increase in nutrient concentrations to values of 1.5 and 0.1 mg/L for TN and TP respectively at BGB1 (Figure 19). Two processes were likely responsible for the increase: a) nutrient-rich zones within the soil profile were reached by the rising water table and b) mobilization of nutrients by major rainfall events towards the end of August 2015. A strong support for the latter was provided by water quality data at BGB2. It was only possible to collect one water quality sample for BGB2, which was at the end of August 2015 in response to major rainfall events (see Figure 13b). The TN and TP concentrations were 6.1 mg/L and 0.29 mg/L respectively. The high nutrient concentration in the water table can affect the assessment of the efficiency of the bioretention basin BF4 that was

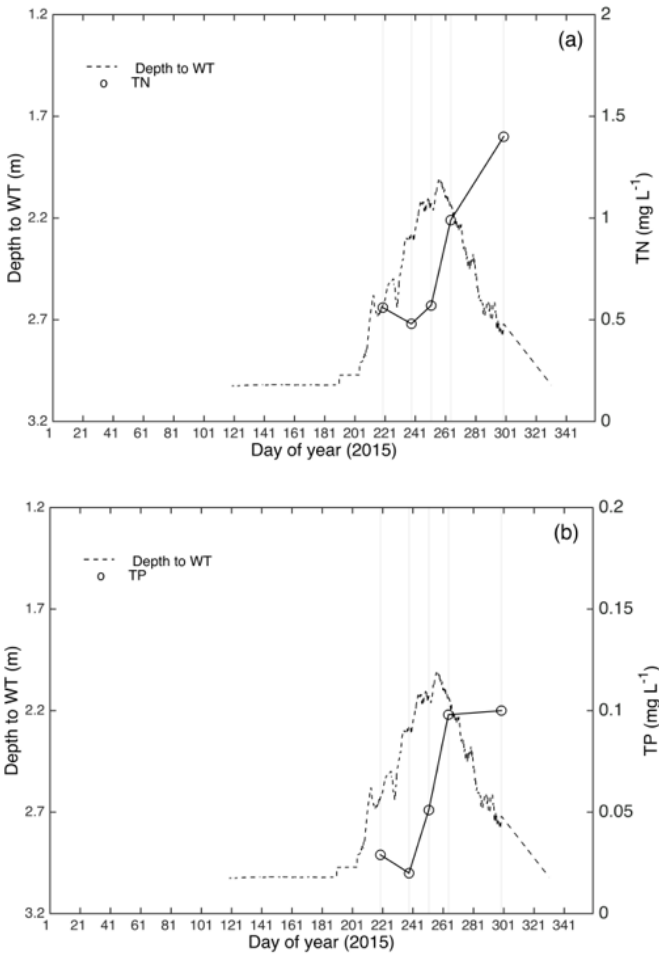

Figure 19: Shallow water table dynamics and nutrient concentrations for BGB1: a) TN and b) TP.

6.2 Raingarden

Concentration values: variability and attenuation

The mean concentrations of nutrient species in the raingarden inflow and outflow for all events are shown in Table 10, and box-plots for the concentration dataset are presented in Appendix 2. Overall, there was a reduction in mean TP concentration by 79%, and mean filterable reactive phosphorus (FRP) entering the system, was reduced by 50%. FRP made up 13% of the TP.

The mean concentration of TN was reduced by 58%. Inorganic nitrogen species (NH3-N and NOx-N) made up < 10% of TN at the inflow, however NOx-N doubled its concentration at the outflow and made up 40% of TN. Dissolved organic nitrogen (DOrgN) made of up 25% of the inflow TN, and experienced a small reduction in concentration at the outflow.

Table 10: Mean nutrient concentrations and its attenuation for nutrients, across all events at the raingarden.

BF1	Inflow			Outflow			
	Mean	Standard Deviation	No Samples	Mean	Standard Deviation	No Samples	Reduction of Mean*
	[mg/L]			[mg/L]			[%]
TP	0.122	0.107	28	0.026	0.011	37	79
FRP	0.016	0.014	28	0.008	0.004	37	50
TN	0.755	0.726	28	0.324	0.134	37	58
NH3-N	0.044	0.087	28	0.012	0.010	37	73
DOrgN	0.179	0.185	28	0.147	0.062	36	18
NOx-N	0.064	0.204	28	0.131	0.083	37	-105
TSS	230	275	23	2	2	33	99

** Reduction of mean (%) calculated using Equation 1 in which EMC is replaced by mean concentration values reported in this table.*

Table 11 shows a comparison of our measured mean concentrations for individual events with the ANZECC (2000) guidelines for estuaries in south-west Western Australia. These guidelines were selected because the ultimate receiving environment for this development is the Peel Harvey Estuary.

Total phosphorus (TP) concentrations were reduced by the raingarden. In all events, as seen in Table 11, the TP mean concentration at the inflow exceeded the ANZECC guidelines, and in all but one event this concentration was reduced to below the guideline value at the outflow. In the one event (20 July 2015) for which the outflow failed to meet the guideline, the raingarden still reduced the mean concentration by 83% and the outflow mean concentration was only just above the guideline value.

FRP reduction was more variable than for TP (Table 11). An average FRP concentration reduction of 67% was achieved for the first four events early in the season when FRP was up to 13% of TP. In contrast, for events in August when FRP was only 5% of TP, outflow mean concentrations were equal to or larger than those at the inflow. The results suggest that FRP reduction is greater at higher FRP concentrations. It is possible that a threshold FRP concentration exists; when inflow concentrations fall below this threshold, effective treatment of FRP will not occur (Wong, 2006).

The mean concentration of total nitrogen (TN) was reduced on average by 50%, with the largest reduction (~80%) achieved for two small events. Only one event (30 August 2015) showed an increase (by 35%) in mean concentration at the outflow. TN at the inflow was above ANZECC guidelines for over half the events, but all outflow mean concentrations were below the guidelines.

Concentrations of ammonia nitrogen (NH_3-N) for the inflow were below the guidelines in all but two events and the same was true for the outflow. As previously noted, ammonia represents a very small fraction of TN (~ 3%) and an average reduction of 68% was achieved for the four first events of the season (Table 11).

Dissolved organic nitrogen (DOrgN) contributed on average 20% and 40% of the inflow and outflow TN concentrations respectively. An average 70% reduction in DOrgN concentrations was achieved for two events early in the season and they were characterised by TN concentration above 2 mg/L. Later in the season the concentration was only reduced by 36%. Underperformance was observed for other events (Table 11). This may be linked to accumulation of DOrgN in the subsurface media that is mobilized by small events with low inflow concentrations.

Unlike other forms of nitrogen, nitrate (NOx-N) showed a different trend. The raingarden acted as a source of NOx-N increasing the mean concentration at times by 100%. The data indicated high variability in mean concentrations and some dependence on event characteristics. Nitrate made up on average 5% of TN in the inflow but it reached 51% of TN mean concentration for the outflow and resulted in outflow concentration values exceeding the ANZECC guideline. Table 11 shows that two events triggered increases in NOx-N of up to 1000%; on 30 August 2015 the mean concentration for the inflow was 0.019 mg/L and 0.25 mg/L for the outflow.

There are a number of possible explanations for this observed behaviour. The raingarden filter media design did not incorporate a saturated anaerobic zone (also known as submerged zone) to facilitate denitrification. This means that it likely provided a suitable aerobic environment for mineralisation of any organic nitrogen retained in the subsurface media, and for nitrification processes (microbial conversion of ammonium to nitrate). The high infiltration rates through the subsurface media during events also indicate aerobic conditions with little variation on mean dissolved oxygen concentrations between inflow (7.8 mg/L) and outflows (7.5 mg/L). The lower than expected nitrate removal by the raingarden with respect to NOx-N may also be due to sub-optimal vegetation performance. Species like Carex possess very high numbers of microscopic root hairs, which greatly increase the area of soil exploitable by the plant (Bratieres et al., 2008). The plants used in the raingardens, though native, may be less than ideal for nitrate uptake. Bratieres et al. (2008) found that vegetation selection was critical for nitrogen removal performance (e.g. Carex appressa and Melaleuca ericifolia performed significantly better than other tested species).

Table 11: Mean concentrations for the raingarden BF1. ANZECC Guidelines (for estuarine protection) are given for nutrients. Numbers in red represent concentration values exceeding the guidelines.

Event		TP	TN	FRP	NOx-N	NH_3-N	DOrgN	TSS
		[mg/L]	[mg/L]	[mg/L]	[mg/L]	[mg/L]	[mg/L]	[mg/L]
ANZECC		0.03	0.75	0.005	0.045	0.04*	n/a	n/a
17/5/15	Inflow	0.230	2.350	0.047	0.615	0.295	0.620	39
	Outflow	0.025	0.440	0.005	0.180	0.012	0.240	7
19/6/15	Inflow	0.096	0.525	0.018	0.020	0.025	0.138	335
	Outflow	0.019	0.320	0.011	0.110	0.017	0.190	2
20/7/15	Inflow	0.210	1.200	0.018	0.045	0.053	0.170	216
	Outflow	0.036	0.640	0.009	0.330	0.013	0.150	5
31/7/15	Inflow	0.430	2.400	0.025	0.030	0.018	0.420	451
	Outflow	0.028	0.400	0.002	0.240	0.005	0.086	4
17/8/15	Inflow	0.098	0.550	0.002	0.067	0.005	0.160	62
	Outflow	0.028	0.440	0.005	0.240	0.015	0.140	2
19/8/15	Inflow	0.190	0.930	0.007	0.014	0.005	0.085	190
	Outflow	0.027	0.280	0.006	0.170	0.005	0.110	3
20/8/15	Inflow	0.120	0.530	0.002	0.012	0.005	0.110	120
	Outflow	0.021	0.200	0.006	0.100	0.005	0.087	1
30/8/15	Inflow	0.042	0.310	0.002	0.019	0.017	0.110	28
	Outflow	0.019	0.420	0.002	0.250	0.017	0.140	1
10/9/15	Inflow	0.245	1.340	0.006	0.030	0.005	0.185	148
	Outflow	0.014	0.270	0.002	0.130	0.005	0.130	1

** Corresponds to un-ionised ammonia-N at 20°C.*

Leaching of NOx-N from biofilters has been previously reported (Hatt et al. 2009). They found that the leaching was exacerbated when there was an extended dry period prior to an event. This allowed the build up of NOx-N prior to the event, and subsequent mobilization that impacted on NOx-N removal efficiencies (Hatt et al., 2009).

Load attenuation

Due to the flow reduction (water mass removal) by the raingarden, the overall performance of the raingarden is better quantified by using nutrient load data and Equation 2 (Table 12).

Load attenuations of up to 95% for TP and 86% for TN were achieved by the raingarden (see Table 12). Note that TN mean concentrations only reduced by about 60% (Table 10). The raingarden attenuated the load of FRP by 72% and of DOrgN by 73%.

The raingarden acted as a source of NOx-N load (Table 12), with the NOx-N load increasing by 81% on average; this was strongly driven by an increase in outflow mean concentrations and outflow discharge during major events (Table 12). By comparing events of similar magnitude occurring in May and late August, we noted that there was a seasonal increase in NOx-N load as the catchment wetted up.

Figure 20 and Figure 21 show TP and TN loads respectively, with the outflow load calculated using time-weighted composite samples (or mean concentration) as well as the "first-flush" water sample for comparison. Of note are the differences in calculated load attenuation (up to 25% on average across all events) when using first-flush bottle and time-weighted composite bottle concentrations to characterise mean concentration values. Differences in load estimates at the outflow were particularly noticeable for the early events of the season from May to July as nutrients stored during the dry period were mobilised. During this time the first-flush bottle filled up early in the event as the threshold volume to initiate outflow from the raingarden was reached and it was not able to capture the extended flow conditions as its full length reached saturation during the large events. This effect was particularly marked for NOx-N (Figure 22) and load was underestimated by 11, 39, and 51% for the first three events respectively. This finding has important implications for monitoring and questions the validity of using single bottle sampling at the outflow at the beginning of the runoff event as representative of mean concentrations throughout the event.

Table 12: Load attenuation for each event at the raingarden (BF1).

Event data	Inflow [L]	Outflow [L]	TP [%]	TN [%]	FRP [%]	NOx-N [%]	NH_3-N [%]	DOrgN [%]	TSS [%]
17/5/15	37758	28832	92	86	92	78	97	70	86
19/6/15	84775	43813	90	68	68	-184	65	29	100
20/7/15	83333	51658	89	67	69	-355	85	45	99
31/7/15	13349	1416	99	98	99	15	97	98	100
17/8/15	27992	2424	98	93	83	69	74	92	100
19/8/15	21461	3326	98	95	87	-88	85	80	100
20/8/15	27841	12045	92	84	-30	-261	57	66	100
30/8/15	20162	3051	93	79	85	-99	85	81	99
10/9/15	15772	182	100	100	100	95	99	99	100
		Average	**95**	**86**	**72**	**-81**	**83**	**73**	**98**

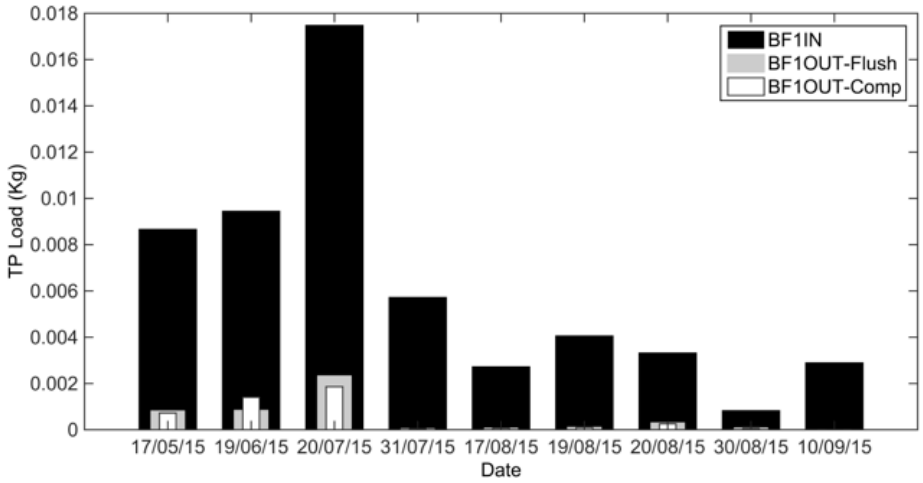

Figure 20: Comparison of TP load estimates for selected events at the raingarden BF1, with two values for the outflow showing the effect of using different concentration values in the load calculation.

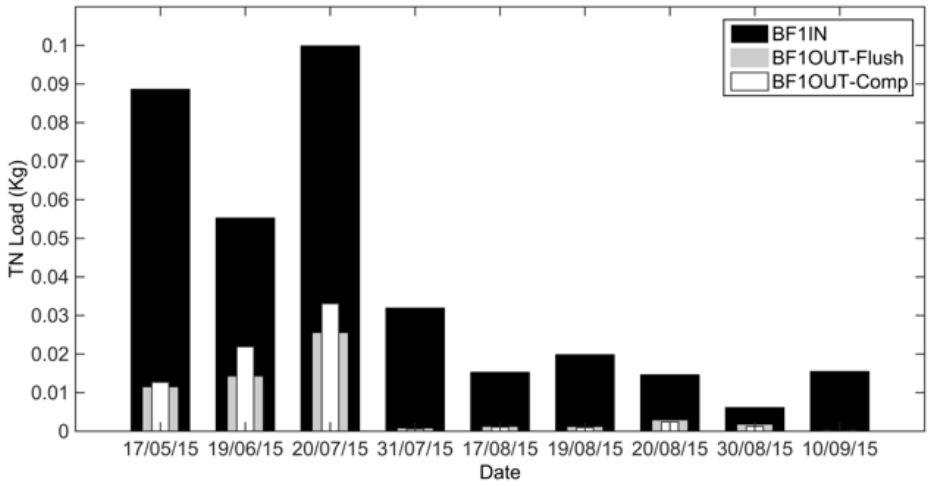

Figure 21: Comparison of TN load estimates for selected events at the raingarden BF1, with two values for the outflow showing the effect of using different concentration values in the load calculation.

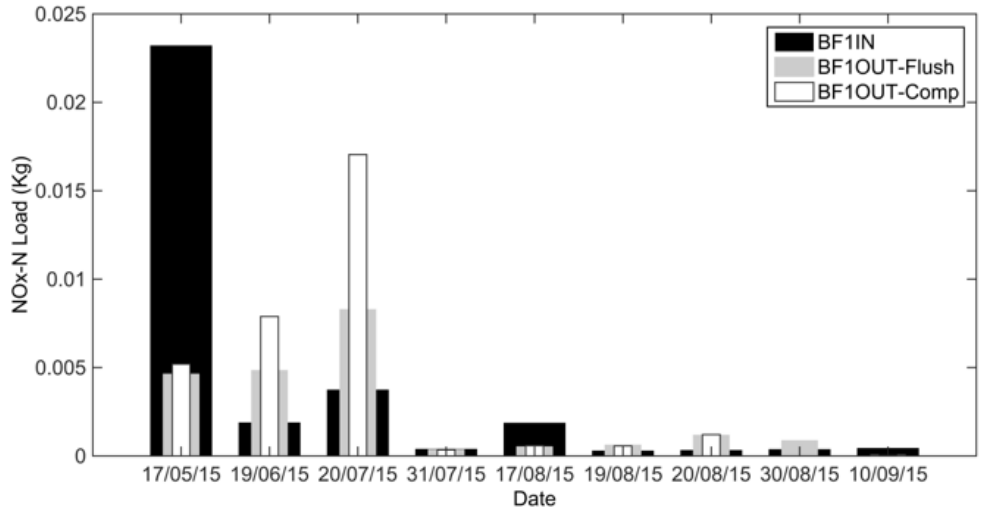

Figure 22: Comparison of NOx-N load estimates for selected events at the raingarden BF1, with two values for the outflow showing the effect of using different concentration values in the load calculation.

The above results suggest that nutrients in particulate form made up a substantial component of the inflow TP and TN concentrations and the decrease in total nutrient concentrations at the outflow could be linked to sediment retention. The raingarden demonstrated effective trapping of suspended particulates; TSS concentrations decreased 99% from the inflow to the outflow (Table 12).

Clogging can occur when fine particles are leached from the media itself (Hatt et al., 2009; Payne et al., 2015) and the transition layer is designed to minimise this effect (Payne et al., 2015). However, five years after installation of the raingarden without a transition layer above the slotted pipe, the raingarden filter media was not showing any signs of clogging. The combination of filter media (Gingin loam) and the vegetation species used appears to be effective at maintaining hydraulic conductivity, with the root growth likely creating sufficient macropores to maintain porosity. This may change in the future and it would be worthwhile investigating.

Is the raingarden effective in removing nutrients?

Load data show that the raingarden is highly effective at total phosphorus and nitrogen removal with load attenuation up to 90 and 80% respectively during the wet season (reaching up to 100% for small events late in the year). This is assumed to be largely due to removal of suspended solids from the stormwater, as well as the volume reduction across the raingarden. Outflow concentrations of TP and TN were reduced to below the guidelines necessary for protection of the receiving estuary.

The raingarden showed a more varied performance with respect to soluble nutrient fractions. Attenuation of FRP mean concentrations was slightly less reliable, and to further reduce FRP concentrations the raingarden could be modified to include the use of a soil media with a higher PRI, or a soil blended with a soil amendment. Examination of overall load data indicates that the raingarden is effectively attenuating FRP load, with an average load reduction of 72% (see Table 12).

The raingarden appears to be ineffective at treating nitrate (NOx-N). This is likely to be due to the lack of a saturated or submerged zone to provide anoxic conditions for denitrification, whereby nitrates can be broken down. Another factor contributing to the lower than expected nitrate removal may be the short residence time of the water through the filtering soil media; this reduces the time NOx-N is exposed to nitrate-reducing microorganisms and plant uptake. Future work should focus on improvement of the raingarden design to tackle this issue.

6.3 Bioretention basin

Concentration values: variability and attenuation

Table 13 presents the statistics for all samples collected over the sampling period at the bioretention basin inflow and outflow. The mean TP concentration at the outflow was 33% lower than the inflow, however TN concentrations at the outflow were 9% higher than the inflow.

A large variability in nitrogen concentrations at the inflow was observed across the season, and with rainfall event characteristics. The mean TN concentration at the inflow station was 0.826 mg/L (± 0.602 mg/L) with a maximum of 2.3 mg/L observed on 28 July during a small runoff event. Higher TN concentrations between 1 and 2 mg/L were commonly observed during large rainfall events that mobilized nutrients from different water sources within the catchment area including the water table, with NOx-N up to 67% of TN. Other nitrogen species showed that on average, DOrgN made up 22% of TN with a number of water samples making up to 47% of TN. Ammonia concentrations were consistently low with no trend over time and mean concentration of 0.026 mg/L (66% of water samples were below the detection limit of 0.01 mg/L.

A seasonal pattern for TP and FRP concentrations was observed at the inflow. The mean TP concentration was 0.027 mg/L (± 0.02 mg/L) with a peak concentration of 0.092 mg/L recorded during a large rainfall event on 20 June. It is interesting to note that FRP concentrations declined over time (to below analytical detection limit = 0.005 mg/L). The mean FRP concentration was 0.008 mg/L (± 0.004 mg/L) and it made up to 47% of TP particularly during events prior to the wet August. Over this time, samples collected during large rainfall events exhibited a FRP/TP ratio of around 10% with high TSS concentrations (39 mg/L), highlighting the mobilization of particulate-P from the catchment by large flows.

The mean TP concentration at the outflow was 0.018 mg/L (± 0.012 mg/L) with a maximum of 0.079 mg/L measured under low flow conditions in early August 2015. The mean FRP concentration was 0.008 mg/L (± 0.005 mg/L) and on average made up 56% of TP. We note that 41% of water samples collected during the late August-October period were below detection limit for FRP. Samples collected over large rainfall events after August presented FRP/TP ratios of around 45%, however in contrast to large events early in the season (before August), the samples contained very low TSS concentrations (←1 mg/L). This suggests that other forms of dissolved P (i.e. dissolved organic P) were being mobilized from the bioretention basin filter media by large flows at this time.

Table 13: Mean concentration and its attenuation of nutrients, across all events at the bioretention basin.

	Inflow			Outflow			
BF4	Mean	Standard Deviation	No Samples	Mean	Standard Deviation	No Samples	Reduction of Mean*
	[mg/L]			[mg/L]			[%]
TP	0.027	0.018	24	0.018	0.012	59	33
FRP	0.008	0.004	24	0.008	0.005	59	0
TN	0.826	0.602	24	0.902	0.613	59	-9
NH_3-N	0.026	0.020	24	0.010	0.009	59	62
DOrgN	0.163	0.141	23	0.214	0.156	55	-31
NOx-N	0.566	0.469	24	0.655	0.497	59	-16
TSS	9	13	14	2	4	25	78

** Reduction of mean (%) computed using equation 1 in which EMC is replaced by mean concentration values reported in this table.*

Table 14 shows a comparison of our measured mean concentrations for individual events with the ANZECC (2000) guidelines for estuaries in south-west Western Australia. Inflow and outflow TN concentrations exceeded guidelines in 58% of events from early August to the end of the monitoring period. NH3-N concentrations exceeded the guideline only for the inflow of a small event on 6 July. In contrast, NOx-N concentrations for inflows and outflows exceeded the guideline for all the events (Table 14). The TP guideline was exceeded at both the inflow and outflow during one event (6 July 2015) while the inflow exceeded the guideline for a major event on 19 August. In contrast the inflow and outflow exceeded the FRP guideline for 75% of the events and these events occurred early in wet season and included the major event on 19 August (Table 14).

In summary, both N and P concentrations showed seasonal trends in response to changing hydrological conditions and functioning of the bioretention basin. Such periods corresponded to changes in VR and the shallow WT levels intercepting the subsoil pipes in the bioretention basin.

Table 14: Mean concentrations for the bioretention basin (BF4) for individual events. ANZECC Guidelines (for estuarine protection) are given for nutrients. Numbers in red represent concentration values exceeding the guidelines.

Event		TP [mg/L]	TN [mg/L]	FRP [mg/L]	NOx-N [mg/L]	NH_3-N [mg/L]	DOrgN [mg/L]
ANZECC		0.03	0.75	0.005	0.045	0.04*	n/a
21/06/15	Inflow	0.023	0.585	0.014	0.360	0.023	0.150
	Outflow	0.032	0.497	0.017	0.309	0.009	0.170
6/07/15	Inflow	0.037	0.230	0.013	0.101	0.046	0.038
	Outflow	0.033	0.660	0.006	0.318	0.021	0.285
20/07/15	Inflow	0.025	0.510	0.009	0.380	0.011	N/A
	Outflow	0.024	0.240	0.010	0.140	0.005	N/A
31/07/15	Inflow	0.019	0.470	0.007	0.420	0.005	0.012
	Outflow	0.015	0.540	0.006	0.440	0.005	0.090
17/08/15	Inflow	0.016	0.863	0.009	0.556	0.013	0.131
	Outflow	0.017	0.746	0.006	0.493	0.005	0.245
19/08/15	Inflow	0.035	1.152	0.006	0.675	0.018	0.300
	Outflow	0.022	0.480	0.007	0.350	0.020	0.101
4/09/15	Inflow	0.018	**1.100**	0.002	0.870	0.005	0.220
	Outflow	0.007	**1.100**	0.002	0.830	0.039	0.180
11/09/15	Inflow	0.014	1.360	0.004	1.090	0.031	0.207
	Outflow	0.010	0.800	0.002	0.560	0.016	0.200
18/10/15	Inflow	0.010	0.520	0.005	0.380	0.005	0.130
	Outflow	0.015	**1.100**	0.002	0.700	0.005	0.370

** Corresponds to un-ionised ammonia-N at 20°C.*

Load attenuation

Calculated load attenuations across each rainfall event are presented in Table 15, and the loads at the inflow and outflow for TN, TP and NOx-N are shown in Figure 23, Figure 24 and Figure 25 respectively. These values need to be interpreted carefully for the bioretention basin, particularly once it intercepted groundwater later in the season.

Overall, the average load attenuation was 33 and 39% for TP and TN respectively. Differences were observed in load attenuation across the range of rainfall event sizes (design, small, minor and major) and season. As an example, we examined in more detail the event on 4 September that was close to design conditions (Table 9); the bioretention basin achieved a 16% volume reduction for the event and water level at the surface storage reached 0.33 m.

For this event, the bioretention basin showed different load attenuations for the different nutrient species (Table 15). The basin achieved 47% attenuation for TP and a much lower value for TN, NOx-N and FRP that were on average at 18% and close to that for volume reduction (16%). Although the NH_3-N load increased markedly across the bioretention basin, the outflow mean concentration was still just below guidelines value (see Table 14).

Also of interest is the difference in load attenuation during the two major events on 21 June and 19 August (Table 15 and Figure 23-25). During the event on 21 June, TP concentration increased by 39%, however, during second event TP load was attenuated by 48%. TN and NOx-N loads were attenuated by 66% and 58% for (Figure 23-25). We note that NOx-N comprised approximately 60% of TN in the second event.

Table 15: Load attenuation for each event at the bioretention basin (BF4).

			Load attenuation [%]					
Event	**Inflow**	**Outflow**	**TP**	**FRP**	**TN**	**NOx-N**	**NH_3-N**	**DOrgN**
data	[L]	[L]	[%]	[%]	[%]	[%]	[%]	[%]
21/06/15	1166424	1071508	-28	-6	22	21	63	-4
6/07/15	370491	332293	20	57	-157	-181	59	-573
20/07/15	244773	206990	19	6	60	69	62	N/A
31/07/15	236370	171200	43	38	17	24	28	-421
17/08/15	535227	424808	14	43	31	30	69	-48
19/08/15	1193070	1136125	47	-1	66	58	9	73
4/09/15	402166	333474	47	17	17	21	-547	32
11/09/15	364788	254822	50	58	59	64	64	33
18/10/15	239255	120522	24	75	-7	7	50	-43
Average			**33**	**42**	**39**	**37**	**50**	**46**

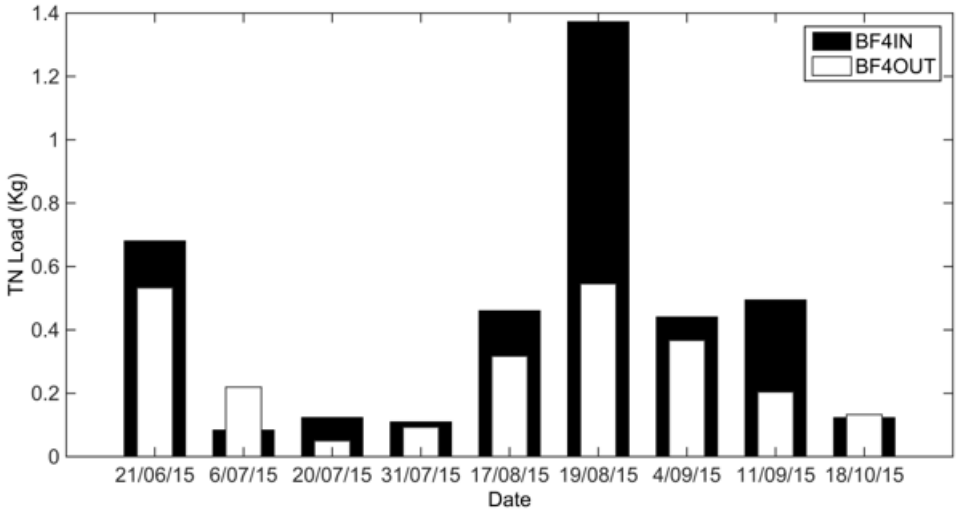

Figure 23: TN load estimates for selected events at the bioretention basin BF4.

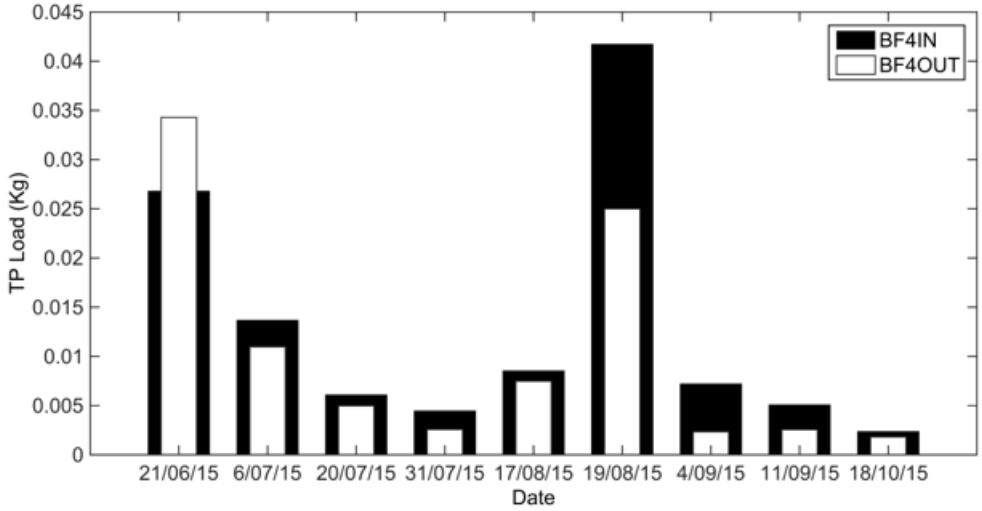

Figure 24: TP load estimates for selected events at the bioretention basin BF4.

The difference in the performance for TP and TN load attenuations may be explained in terms of the hydraulic functioning of the basin under different hydrological and hydraulic conditions. Dry conditions prevailed prior to the first major event; sediment was available for transport and cracks were observed in the soil surface and subsurface within the basin, creating preferential flow pathways. These conditions allowed sediment and nutrients to reach the outflow pipe with limited contact with the filter media. The load reductions achieved for TN and NOx-N over this first event were similar to water losses; at this time the water table was not developed and did not interact with the basin. In contrast, the second event occurred under wet antecedent conditions and the water table by this time in the season was intersecting the outflow pipes.

The high attenuation of TN load could be the result of interaction with the water table, which had lower TN concentrations (0.48 mg/L) than the surface inflows for this event (see Figure 23). There could have been dilution of NOx-N from rainfall on previous days. First flush samples at the outflow consistently showed that NOx-N made up 75% to 100% of TN. NH_3-N load attenuation was around 63% for the first event, but it dropped to 9% for the second and then the bioretention basin became a source of NH_3-N for the subsequent event (Table 15).

Load attenuation of N and P over frequent small events (5-14 mm) displayed differences depending on the season and the presence of the water table. For example, TP attenuation was 47% and 50% for two events experiencing 30% reduction in water volume (see Figure 24, events 31/07 and 11/09) but showed FRP attenuation at 38% and 58% respectively (Table 15). The difference could be explained by dilution from water table discharge with a low FRP concentration (below analytical detection limit). TN and NOx-N attenuation also showed significant differences between the two events (Table 15) and displayed an improvement from 17% to 59% for TN (Figure 23) and from 24% to 64% for NOx-N (Figure 25) over the first and second events respectively. The latter occurred close to the time of the water table peak and presented low TN concentration (see Section 4.1, Figure 19a).

The effect of the water table on bioretention basin performance can be illustrated by the event on 18 October, when high TN and NOx-N concentrations were found in the outflow (Table 14). The low load attenuation for TP, TN, and NOx-N contrasted with the 75% attenuation observed for FRP. The water and nutrient balance for the event explains the low attenuation for TN and NOx-N (Table 15, Figure 23 and Figure 25). Over this event, 50% of the inflow was lost and water table contributions made up 25% of the outflow. An inverse calculation of the nutrient mass balance predicted water table TP and TN concentrations of 0.03 mg/L and 2.8 mg/L respectively, which were similar to those observed in the baseflow over the days prior the event, and in the

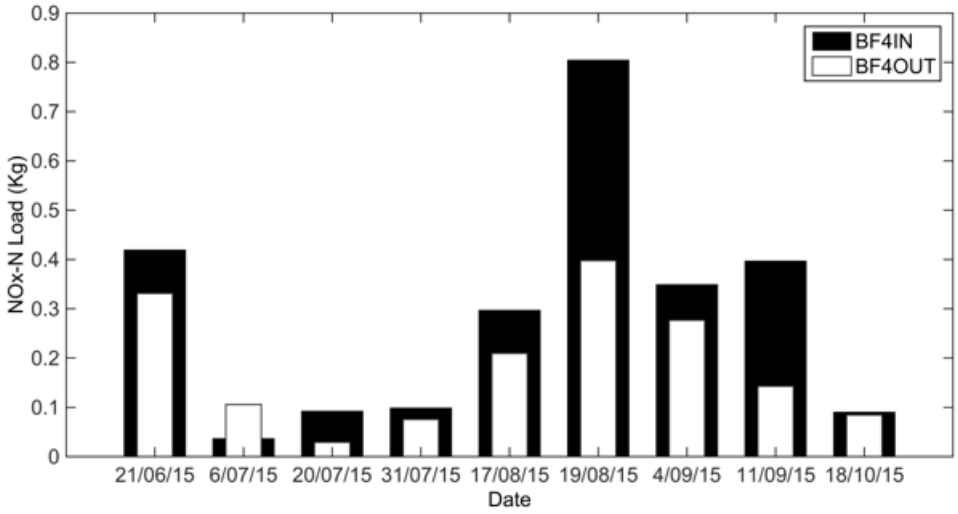

Figure 25: NOx-N load estimates for selected events at the bioretention basin BF4.

first-flush samples from the bioretention basin (range 1 - 2.8 mg/L for TN). The poor attenuation of TN was also likely driven by the 35% increase in DOrgN concentration measured at the outflow.

Is the bioretention basin effective in removing nutrients?

Nutrient load data show that the bioretention basin is strongly affected by seasonality of water inputs, the interaction with the water table and the nutrient species and fractions. There was substantial removal of suspended solids from the stormwater; this improved TP load attenuation however as dissolved species make up most of the TN this did not benefit TN load attenuation.

The average TP and TN load attenuations were 33% and 39% respectively. Over a seasonal scale, different mechanisms appeared to control attenuation and all were related to the presence of the water table. High load attenuation in the basin corresponded to times when the water table was at its highest level, its nutrient concentrations were low and it contributed significantly to the outflow volume. This was also observed for FRP. In contrast, a decline in load attenuation of dissolved nitrogen species occurred as the water table receded and higher concentrations were measured in the water table.

Despite variable load attenuations in the bioretention basin, the load of TN and dissolved nitrogen fraction out of the basin increased over the season as the water table intersected the subsoil pipes and contributed water with higher nutrient concentrations to the outflow. This resulted in concentrations of TN and NOx-N largely exceeding the ANZECC (2000) guideline for estuaries. This issue requires further investigation to identify whether the filter media itself becomes a nutrient source, or other processes are responsible for this seasonal mobilization.

7. Conclusions and recommendations

7.1 Summary of findings

The system

1. There was no direct interaction between the water table and the raingarden outflow pipes, however, the high water table in the wet season decreased infiltration rates from the raingarden. The water table was well above the invert of the stormwater pits at Mead Street and was effectively contributing to the flow of the main drainage network and intercepting the bioretention basin outflow pipe for a period of approximately 50 days. This impacted nutrient attenuation in the bioretention basin.

The raingarden

Did the raingarden attenuate stormflow volumes?

2. A threshold volume of 13.25 m^3 was required to initiate outflow from the raingardens, and 19.1 m^3 to wet up the entire length of the raingarden. Further, a total volume of 31 m^3 was required to generate surface gully overflow. The dosing trial and monitored events showed that the raingarden attenuated stormflow volumes by 68% on average, and by 89% for peak flows.

3. Volumetric ratio values (VR = Volout/Volin) were between 65 to 77% for rainfall events exceeding 40 mm. In general, events of less than 20 mm resulted in a VR from 26 to 48% with the higher value corresponding to a high intensity event (imax_10 = 31 mm/h) on 1 February. A VR of 20% was obtained for an isolated event of 17.8 mm (imax_10 = 42 mm/h), which is close to the 1-year ARI 1-hour event. All events recorded after day 251 (10 September) had rainfall amounts of less than 20 mm and VR values from 0.2 to 12%.

4. Averaging across all rainfall events, 37% of the inflowing water became subsurface outflow runoff, 38% became local recharge (leakage) and 25% became incorporated into soil moisture, which was therefore available for the vegetation and evaporative losses.

5. The combination of filter media (Gingin loam) and the vegetation species used appears to be effective at maintaining hydraulic conductivity, with the root growth likely creating sufficient macropores to maintain porosity. This may change in the future and it would be worthwhile investigating.

Were nutrient concentrations discharged by the raingarden below ANZECC Guidelines?

6. Outflow concentrations of TP and TN were reduced to below the ANZECC guidelines. The raingarden showed a more varied performance with respect to soluble nutrient fractions. Attenuation of FRP mean concentrations was slightly less reliable, and it is likely that to reduce FRP concentrations to below the ANZECC (2000) guideline for estuaries (< 0.005 mg/L), the raingarden would need to be modified. The use of a soil with a higher PRI, or a soil blended with a soil amendment product might be considered.

7. Across the year, there was a reduction in mean TP concentration by 79%, and mean filterable reactive phosphorus (FRP) concentration by 50%. FRP made up 13% of the TP.

8. The mean concentration of TN was reduced by 58%. Inorganic nitrogen species (NH_3-N and NOx-N) made up ← 10% of TN at the inflow, however NOx-N doubled its concentration at the outflow and made up 40% of TN. Dissolved organic nitrogen (DOrgN) made up 25% of the inflow TN, and experienced a small reduction in concentration at the outflow.

Was the raingarden effective in removing nutrients?

9. Over the season, the raingarden was highly effective at TP load attenuation (up to 90%). This is likely due to efficient removal of suspended solids from the stormwater, as well as the volume reduction across the raingarden. The FRP load attenuation was on average 72%.

10. Over the season, the raingarden attenuated TN load well (86%). However it appears to be ineffective at treating nitrate (NOx-N). This is likely to be due to the lack of a saturated or submerged zone to provide anoxic conditions for denitrification, whereby nitrates can be broken down. Another factor contributing the poor performance may be the short residence time of the water through the filtering soil media; this reduces the time NOx-N is exposed to nitrate-reducing microorganisms and plant uptake. Future work should focus on identifying nitrate sources within the raingarden and the improvement of the raingarden design to tackle this issue.

Bioretention basin

Did the bioretention basin attenuate stormflow volumes?

11. In general, outflows and consequently volumetric ratio values (VR) were highly dependent on two factors: the ponding area contributing to infiltration and antecedent conditions.

12. There were important seasonal changes in the underlying hydrology of the area, characterised by frequent rainfall events (< 10 mm) with an average VR value of 20.5% until early June. VR increased to 63.2 % over the period July-mid September, and then dropped back to 20.6% from October to November 2015. A similar seasonal pattern for VR values was observed for events in the 20-30 mm range as average values increased from 48% to 80% over the same period. As expected, large events (→ 40 mm) always showed high VR values, on average around 93%.

13. High VR values over the winter period may reflect an important shift in the subsurface hydrology of the area and potential interaction with the shallow water table.

14. During early events in the season (January and July; 7 mm to 40 mm), residual saturation (water held at the bottom of the bioretention basin filter media) contributed on average 21% (± 6%) of the total event flow (no water table was developed at this stage). As the water table developed, its contribution to the outflow was estimated to be on average 18% (± 7.7%).

Were nutrient concentrations discharged by the bioretention basin below ANZECC Guidelines?

15. NOx-N concentrations for inflows and outflows exceeded the ANZECC guideline for all events. FRP concentrations for inflows and outflows exceeded the ANZECC guideline for 75% of the events and these events occurred early in wet season and included the major event on 19 August.

16. Both N and P concentrations showed seasonal trends in response to changing hydrological conditions and functioning of the bioretention basin.

17. Early in the season, FRP made up 56% of TP, and the high TSS concentrations suggested that particulate P likely made up the difference. In contrast, later in the season FRP made up approximately 45% of TP in large rainfall events however TSS concentrations were very low. At this time of the year, dissolved organic phosphorus likely made up the difference, possibly being mobilized from the bioretention basin filter media.

18. The effect of the water table on bioretention basin performance was illustrated by the event on 18 October, when high TN and NOx-N concentrations were found in the outflow. The relatively low load attenuation for TP, TN, and NOx-N contrasted with the 75% attenuation observed for FRP.

Was the bioretention basin effective in removing nutrients?

19. The load attenuation of the bioretention basin was strongly affected by seasonality in water inputs, the interaction with the water table and the nutrient species and fractions considered for treatment.

20. There was substantial removal of suspended solids from the stormwater; this improved TP load attenuation however as dissolved species make up most of the TN, this did not impact TN load attenuation.

21. The average TP and TN load attenuations were 33 and 39% respectively. Over the season, different mechanisms appeared to control attenuation and all were related to the presence of the water table. High load attenuation in the basin occurred when the water table was at its highest level, its nutrient concentrations were low and it contributed significantly to the outflow volume. This was also observed for FRP. In contrast, a decline in load attenuation of dissolved nitrogen species occurred as the water table receded and high concentrations were measured in the water table.

22. The load of TN and dissolved nitrogen fractions out of the basin increased over the season, as the water table intersected the subsoil pipes and contributed to the outflow. This resulted in concentrations of TN and NOx-N largely exceeding the ANZECC (2000) guidelines. This issue requires further investigation to identify whether the filter media itself becomes a nutrient source, or other processes are responsible for this seasonal mobilization.

7.2 Conclusions

Nitrogen versus phosphorus attenuation

The raingarden consistently attenuated phosphorus loads more effectively than nitrogen loads but load attenuations for both were similar to those measured in the bioretention basin. Particulate phosphorous made up a significant proportion of TP and was effectively trapped by both systems. Both systems were well oxygenated and under those conditions the filter media was effective at attenuating FRP loads.

The nitrogen dynamics were more complex. While TN loads were on average attenuated by both systems, there was variability across the year and they exhibited periods of poor attenuation of NOx-N. This was likely due to the oxic conditions that were maintained in the filter media. In the bioretention basin, these oxic conditions were likely maintained by the low travel times of subsurface drain inflows.

The raingarden

The raingarden performed well under all monitored conditions. It attenuated storm flows as designed. While groundwater did not discharge directly into the raingarden, it did impact it; as the water table rose over the season, the infiltration rate from the raingarden decreased. The raingarden also reduced total nitrogen and total phosphorous to below ANZECC target concentrations and attenuated total nutrient loads by 80 – 90%. Ammonia concentrations were consistently reduced to below ANZECC Guidelines (for estuaries). FRP concentrations were not always reduced to below ANZECC estuarine guidelines, though were below ANZECC lowland rivers guidelines. Nitrate concentrations were consistently higher at the outflow than the inflow, and nitrate was released by the raingarden (loads exiting were higher than loads entering).

The bioretention basin

The dynamics of the bioretention basin were more complex than the raingarden, and it exhibited strong seasonality related to the interception of the water table around August. During this period, the high water table contributed up to 20% of the outflows and the interception of the water table also impacted the nutrient attenuation dynamics; overall TN and TP nutrient load attenuations of 33-39% were lower than measured at the raingarden.

The basin consistently attenuated both TN and NOx-N loads over the year, however nitrate concentrations were above the ANZECC guidelines throughout the year and the outlet nutrient concentrations were strongly affected by the nutrient concentrations in the superficial groundwater. After August and over a period of 50 days (when the water table impacted the basin) TN concentrations were consistently above the ANZECC guidelines. Dissolved organic nitrogen concentrations were also higher at the outflow than the inflow, and at times the basin was discharging significant loads of DOrgN.

7.3 Recommendations

Ideally biofilters provide a range of redox conditions for optimal nutrient attenuation; this occurs readily in systems with lower permeability soils and higher organic matter content that experience frequent rainfall throughout the year. Biofilters installed in urban areas in Perth experience hot and dry summers, a water table and high permeability soils. These maintain oxic conditions in the biofilter media during the summer season. Winter rains and higher water tables may increase the degree of surface soil saturation, however the high soil permeability and rapid subsurface travel times (exacerbated by subsurface drainage) inject oxygen into the system. This oxygen dynamic and resulting redox conditions have a profound impact on phosphorus and nitrogen attenuation; phosphorus is attenuated effectively under oxic conditons while nitrogen is not. When a single system (whether a raingarden or a bioretention basin) aims for attenuation of both nitrogen and phosphorus, there will always be challenges in how to maintain the optimal redox conditions.

Instead of viewing each biofilter as a nutrient attenuation system, we recommend that:

1. A treatment train approach is used across the catchment, to provide a range of redox conditions for nutrient attenuation;

2. Design to maximize the travel time of subsurface flows across the catchment, and through the filter media.

3. Consider the placement of smaller biofilters throughout the catchment, including in the upland areas to enhance infiltration, increase subsurface travel times and increase the likelihood of nutrient attenuation.

4. Consider alternating surface and subsurface treatment trains across the catchment to provide a range of redox conditions.

8. References

ANZECC & ARMCANZ (Australian New Zealand Environment Conservation Council & Agricultural and Resource Management Council of Australian and New Zealand), (2000). National water quality management strategy: Australian and New Zealand water quality guidelines for fresh and marine water quality. Vol 1, the Guidelines (Chapters 1-7).

BOM (Australian Bureau of Meteorology) (2015). Climate data Online for Cardup Station (Station number: 009137): Daily rainfall data. Accessed at http://www.bom.gov.au/climate/data/index.shtml.

Bratieres, K., T.D. Fletcher, A. Deletic and Y. Zinger (2008). Nutrient and sediment removal by stormwater biofilters: A large-scale design optimisation study, Water Research 42 (2008) 3930– 3940

Burns, M. J, T. D. Fletcher, C. J. Walsh, A. R. Ladson and B. E. Hatt (2015). Flow-regime management at the urban land-parcel scale: test of feasibility. Journal of Hydrologic Engineering (ASCE). DOI:10.1061(ASCE)HE.1943-5584.0001002.

Coffey Geotechnics (2007). Geotechnical Investigation: Byford. Technical Report: GEOTHERD08278AA-AA, July 2007, pp 70.

Dawdy D.R., J.C. Schaake Jr. and W.M. Alley (1978). User guide for distributed routing rainfall-runoff model. US Geological Survey. Water-Resources Investigations 78-90. pp 152.

DoW (Department of Water of Western Australia) (2004). Stormwater Management Manual for Western Australia - Performance Monitoring and Evaluation.

EPA (Environmental Protection Authority) (2008) Water Quality Improvement Plan for the Rivers and Estuary of the Peel-Harvey System - Phosphorus Management, Environmental Protection Authority, Perth, Western Australia.

FAWB (2009). Adoption Guidelines for Stormwater Biofiltration Systems, Facility for Advancing Water Biofiltration, Monash University, June 2009.

Hatt, B. E., T. D. Fletcher and A. Deletic (2009). Hydrologic and pollutant removal performance of biofiltration systems at the field scale. Journal of Hydrology, 365(3-4): 310-321.

JDA Hydrologist Consultants (2009). The Glades, Byford Local Structure Plan Appendix 7 - Local Urban Stormwater Management Report, prepared for LWP Property Group Ltd, by JDA Consulting, June 2009. Li, R.M., D. B. Simons and M.A. Stevens (1975). Nonlinear kinematic wave approximation for water routing. Water Resources Research; 2:245-252.

Lighthill M.J. and G. B. Whitham (1955). On kinematic waves. I. Flood movement in long rivers. Proceedings of the Royal Society. 229: 281- 316.

Payne E.G.I., B . Hatt, A. Deletic, M Dobbie, D. McCarthy D and G. Chandrasena (2015). Adoption Guidelines for Stormwater Biofiltration Systems, Melbourne, Australia: Cooperative Research Centre for Water Sensitive Cities.

Pellerin, B. A., W. M. Wollheim, X. Feng and C.J. Vörösmarty (2008). The application of electrical conductivity as a tracer for hydrograph separation in urban catchments. Hydrological Processes, 22:1810-1818.

Seah, T. (2011). A preliminary investigation of readily available local soils that are suitable filter media for biofiltration systems in Western Australia, Honours Thesis, UWA. Accessed at: http://www.web.uwa.edu.au/__data/assets/pdf_file/0008/1835486/Seah-T-thesis-2011.pdf

Sidoti, D. (2015). Water Sensitive urban Designs: The effectiveness of bioretention basins in areas of significant groundwater interference, Masters Professional Engineering Thesis, University of Western Australia

Sklash, M.G. and R.N. Farvolden (1979). The role of groundwater in storm runoff, Journal of Hydrology, 43, 45-65.

USDA (United States Department of Agriculture) (1986). TR55 Technical Release N 55. Urban Hydrology for Small Watersheds. Second Edition, pp 165.

Winer, R. (2000). National Pollutant Removal Database for Stormwater Treatment Practices. Second edition. Center for Watershed Protection. Ellicott City, MD.

Wong, T.H.F, (2006). Australian Runoff Quality: A Guide To Water Sensitive Urban Design. Sydney, Engineers Australia.

9. Appendices

Appendix 1A – Event hydrographs for raingarden BF1

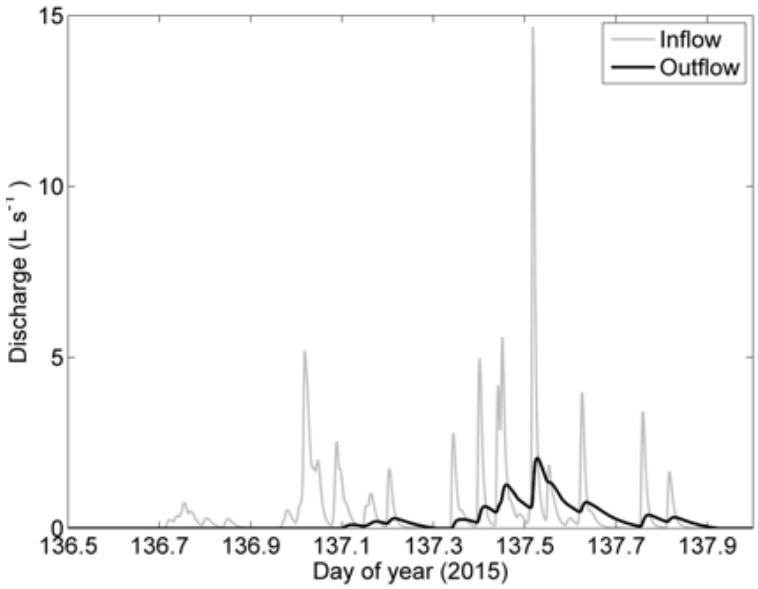

Figure 26: Event on 16 June and 17 May. Total rainfall of 30.6 mm.

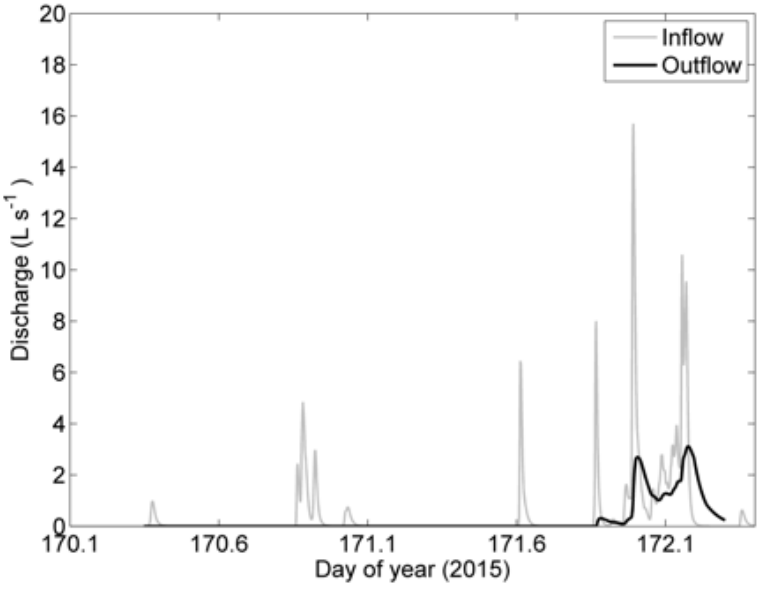

Figure 27: Event on 19 June and 20 June. Total rainfall of 40.8 mm.

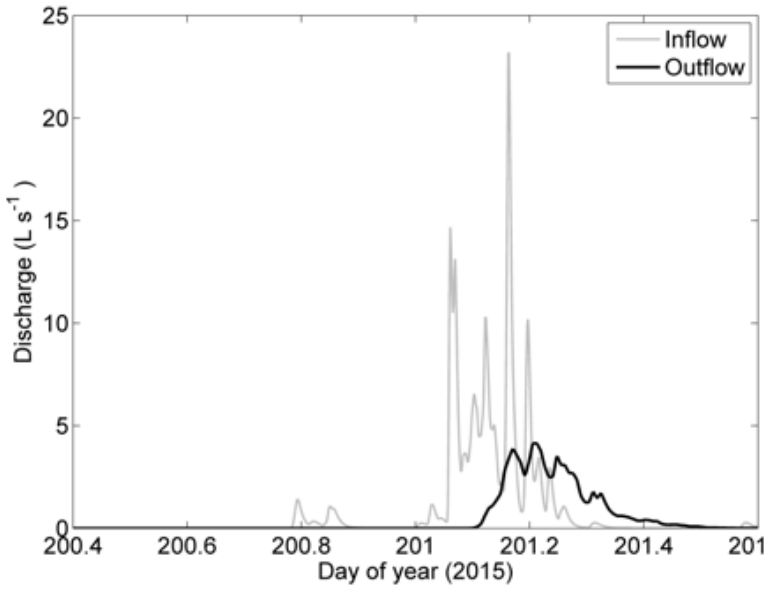

Figure 28: Event on 19 July and 20 July. Total rainfall of 43.6 mm.

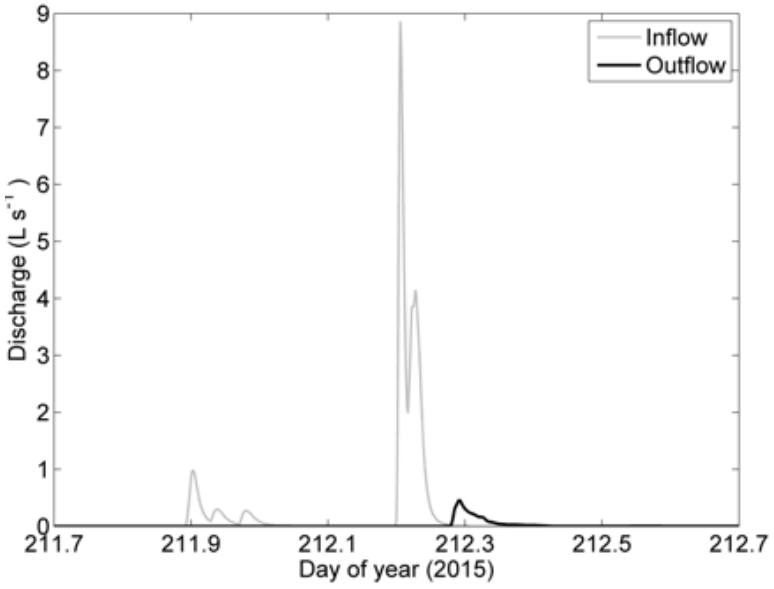

Figure 29: Event on 31 July. Total rainfall of 6.8 mm.

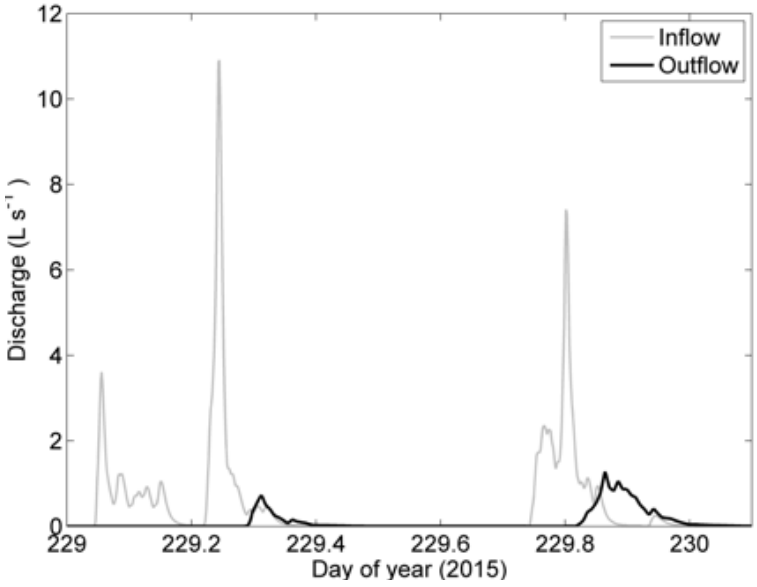

Figure 30: Events on 17 August and 18 August. Total rainfall of 22.8 mm.

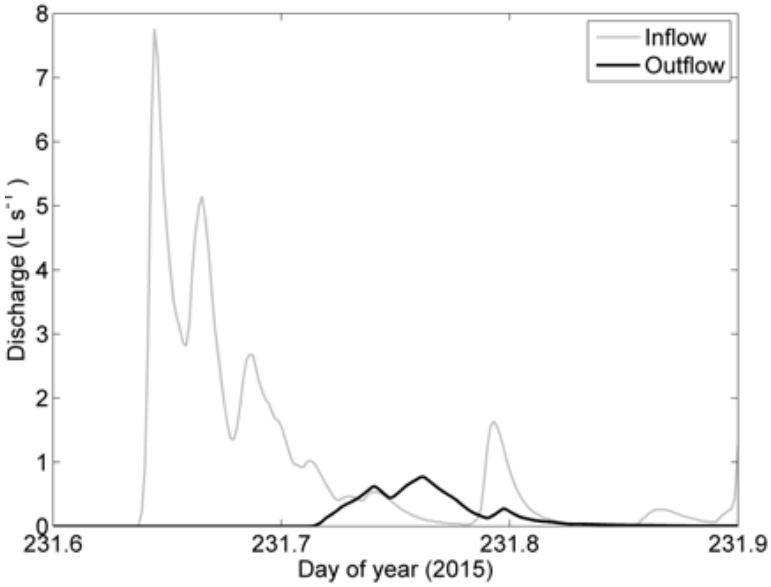

Figure 31: Event on 19 August. Total rainfall of 13.8 mm

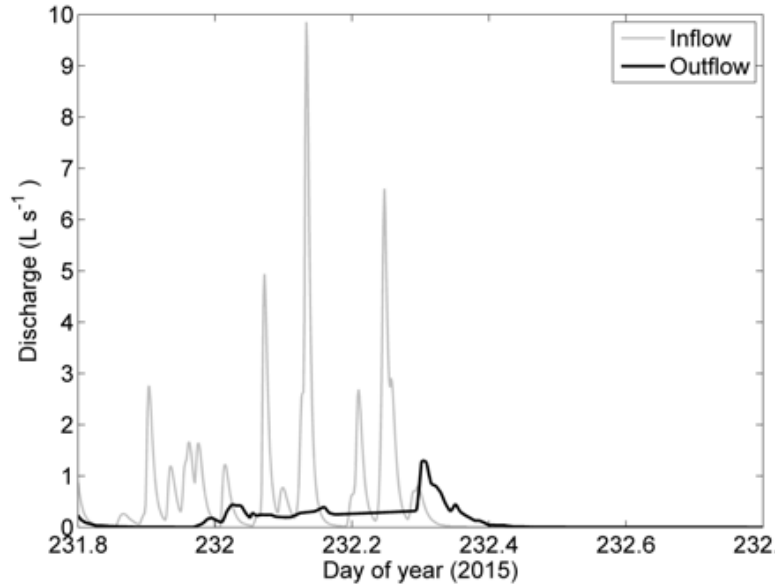

Figure 32: Event on 20 August. Total rainfall of 13 mm.

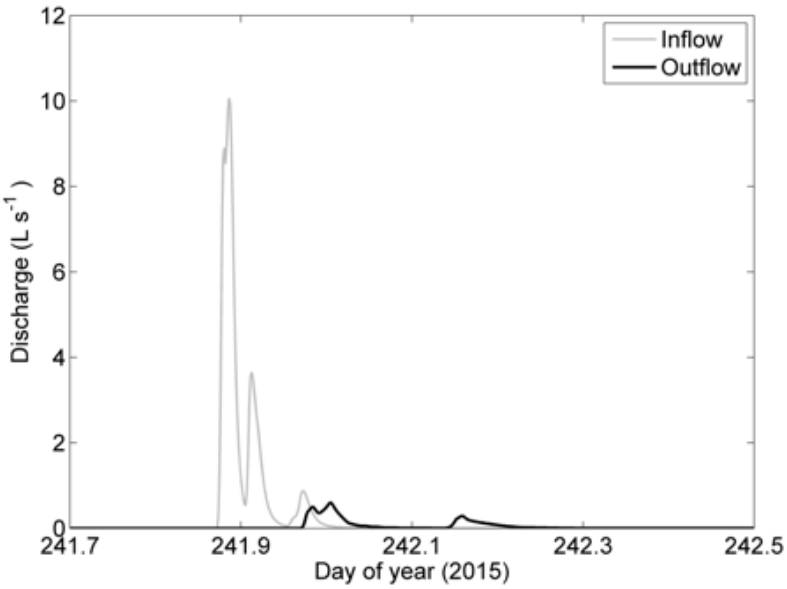

Figure 33: Event on 29 August. Total rainfall of 9.8 mm.

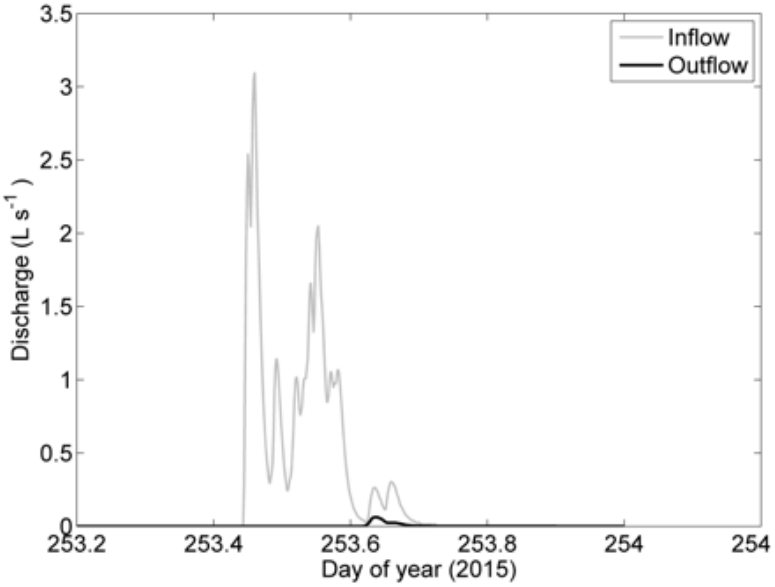

Figure 34: Event on 10 September. Total rainfall of 7.8 mm.

Table 16: Summary of rainfall event characteristics and water balance model outputs for raingarden BF1. Note that inflow and outflow volume values (Vol_in and Vol_out) differ from those reported on Section 5.1, Table 8, as the latter were associated to periods of available water quality data for nutrient efficiency computation.

Date	Day of Year	Total Rainfall	1 Hour Rainfall	Imax_10	ARI	Vol_in	Vol_out	Recharge	Available EV-Loss
	(1/1/15)	(mm)	(mm)	(mm/h)		(m^3)	(m^3)	(m^3)	(m^3)
29/01/15	29	7.0	2.4	9.0	<1	9.461	0.0000	1.716	7.740
1/02/15	32	23.4	10.1	31.2	<1	35.645	17.512	9.140	7.870
14/03/15	73	10.8	4.4	37.4	<1	12.891	0.0000	3.084	7.740
18/03/15	77	6.4	1.8	7.2	<1	10.173	0.0000	2.420	7.748
9/04/15	99	21.6	3.6	13.2	<1	34.716	11.289	11.436	7.870
12/04/15	102	2.6	1.6	8.4	<1	3.105	0.0000	0.0000	3.105
3/05/15	123	11.9	4.0	9.6	<1	18.901	0.0490	7.332	7.870
16/05/15	136	30.6	5.6	24.0	<1	49.834	28.780	7.536	7.870
18/05/15	138	2.8	1.2	4.8	<1	3.066	0.0000	7.320	7.740
2/06/15	153	14.8	5.4	10.8	<1	22.063	0.1690	9.948	7.870
19/06/15	170	40.8	9.2	27.6	<1	68.250	44.643	7.716	7.870
21/06/15	172	20.4	8.8	28.8	<1	34.819	26.789	10.368	7.870
4/07/15	185	9.4	5.4	21.6	<1	13.837	0.0165	2.770	7.870
6/07/15	187	19.4	7.0	13.2	<1	30.331	14.428	4.788	7.870
19/07/15	200	43.6	12.4	37.2	<1	74.420	52.920	4.656	7.870
20/07/15	201	9.8	3.8	10.8	<1	16.170	8.425	8.640	7.870
23/07/15	203	6.2	5.6	8.4	<1	9.595	4.670	3.880	7.870
31/07/15	212	12.0	6.2	19.2	<1	15.057	1.449	1.400	7.870
8/08/15	220	19.6	8.0	22.8	<1	33.960	11.560	14.700	7.710
10/08/15	222	5.0	2.0	8.4	<1	5.759	0.079	0.0000	7.870
17/08/15	229	22.8	6.8	18.0	<1	38.384	9.863	10.800	7.749
19/08/15	231	26.8	6.8	18.0	<1	46.103	26.177	11.500	7.870

Date	Day of Year	Total Rainfall	1 Hour Rainfall	Imax_10	ARI	Vol_in	Vol_out	Recharge	Available EV-Loss
	(1/1/15)	(mm)	(mm)	(mm/h)		(m^3)	(m^3)	(m^3)	(m^3)
21/08/15	233	16.2	9.0	30.0	<1	28.114	19.834	4.900	7.870
29/08/15	241	9.8	8.6	19.2	<1	16.239	3.141	5.300	7.870
31/08/15	243	4.0	2.4	10.8	<1	5.840	0.0000	4.308	7.870
4/09/15	247	17.8	14.0	42.0	~1	29.729	5.906	7.690	7.690
10/09/15	253	7.8	3.4	12.0	<1	15.750	0.181	4.300	7.870
11/09/15	254	14.0	3.4	16.8	<1	22.590	2.612	17.600	7.722
14/10/15	287	6.2	3.2	18.0	<1	7.918	0.000	0.108	7.738
18/10/15	291	11.6	5.4	10.8	<1	19.735	0.097	11.910	7.720
29/10/15	302	14.8	6.4	10.8	<1	23.540	1.122	14.490	7.740
1/11/15	305	7.8	1.6	8.4	<1	10.973	0.000	2.976	7.745
18/11/15	321	5.0	3.4	18.0	<1	5.762	0.000	0.000	4.589
4/12/15	338	17.4	4.8	9.6	<1	26.825	0.059	7.416	7.739

Note: Day of the year since January 1st 2015. I max_10 indicates maximum rainfall intensity over 10 min interval. ARI (Average Recurrence Interval) value corresponds to Imax_10. Recharge volumes accounted over the duration of the rainfall event. Available water for evaporation (EV-loss) after the event.

Appendix 1B – Event hydrographs for bioretention basin BF4

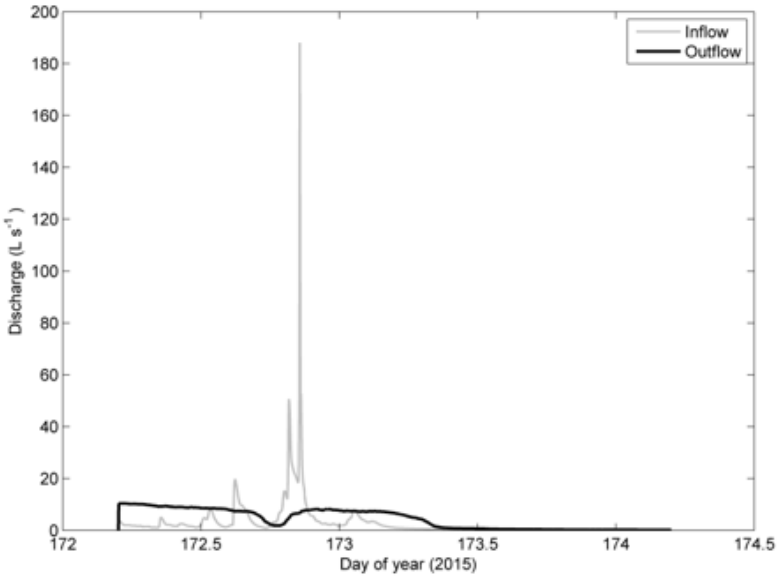

Figure 35: Event on 21 June. Total rainfall of 20.4 mm.

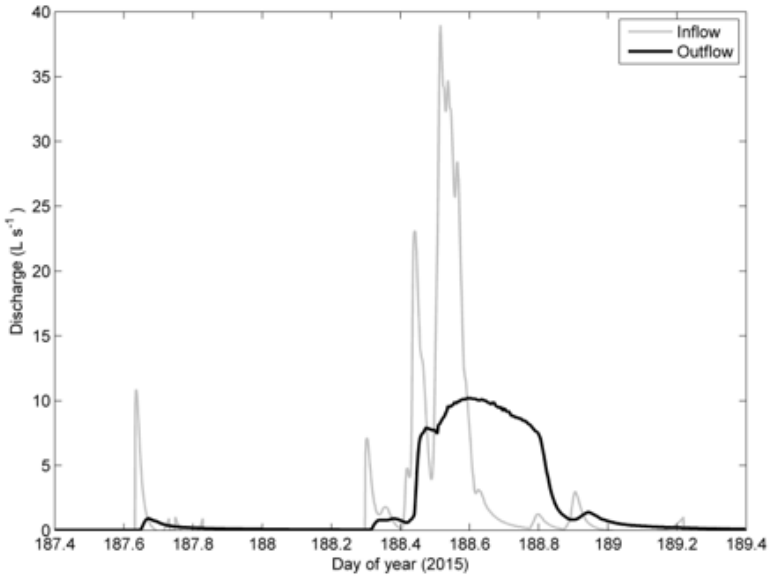

Figure 36: Event on 6 July. Total rainfall of 19.4 mm.

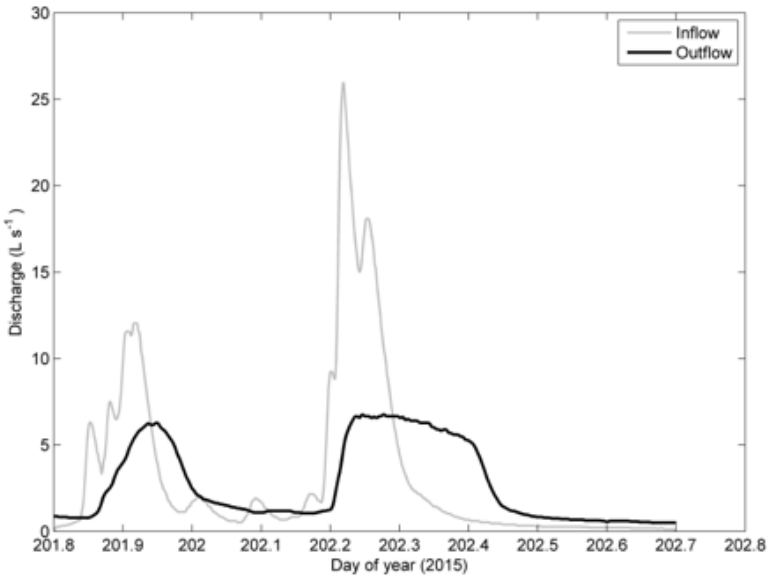

Figure 37: Event on 20 July. Total rainfall of 9.8 mm.

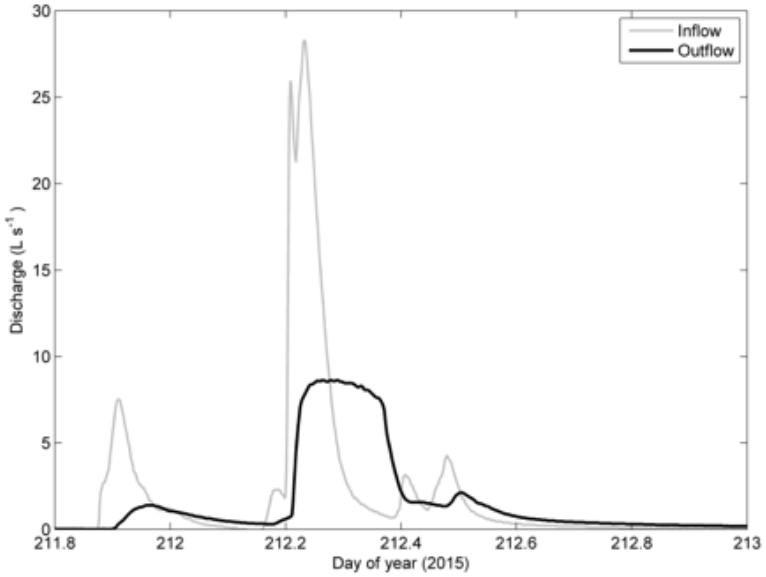

Figure 38: Event on 31 July. Total rainfall of 12 mm.

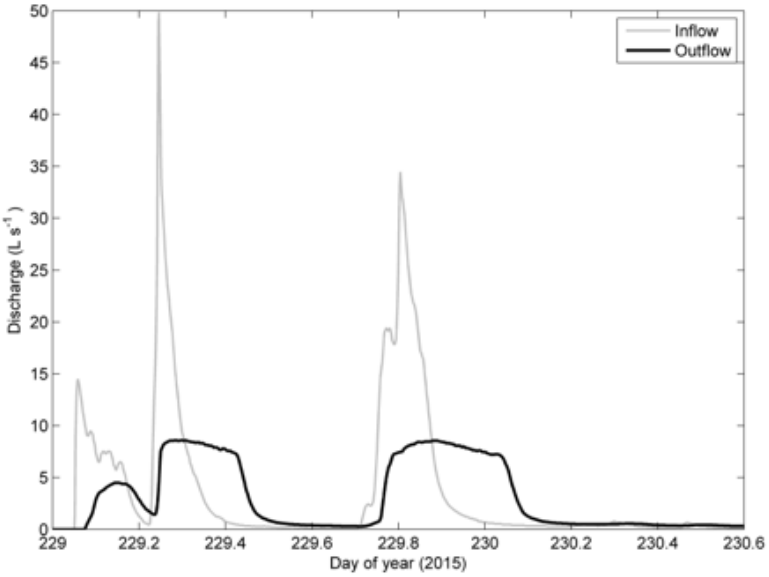

Figure 39: Event on 17 August. Total rainfall of 22.8 mm.

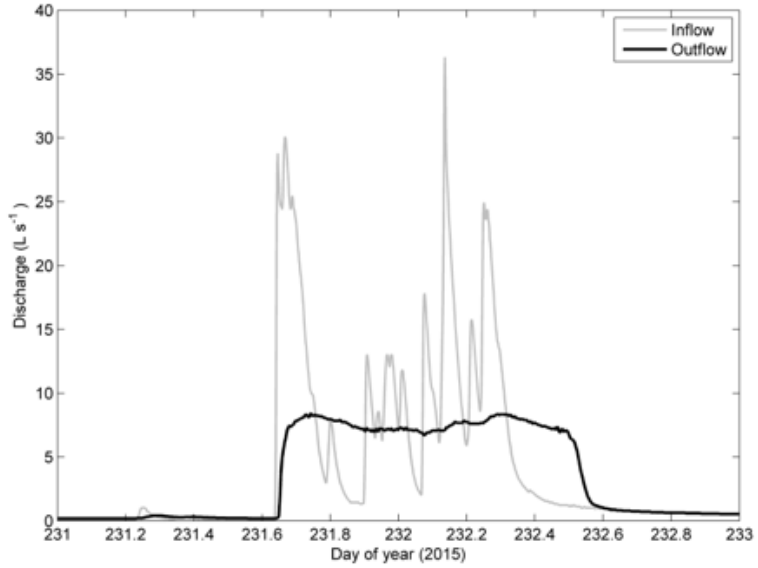

Figure 40: Event on 19 August. Total rainfall of 26.8 mm.

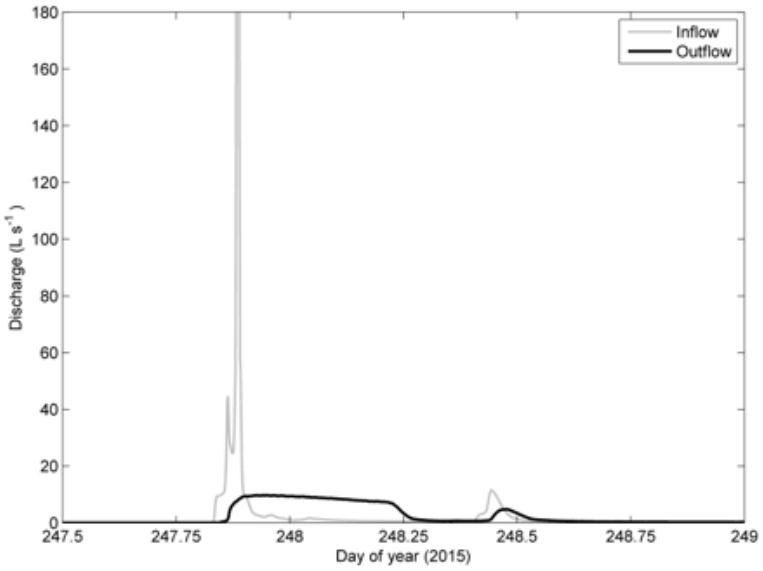

Figure 41: Event on 4 September. Total rainfall of 17.8 mm.

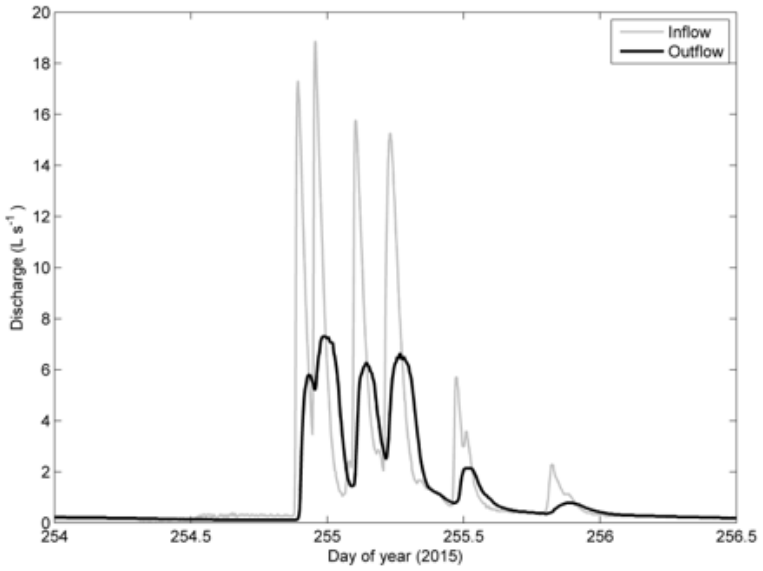

Figure 42: Event on 11 September. Total rainfall of 14 mm.

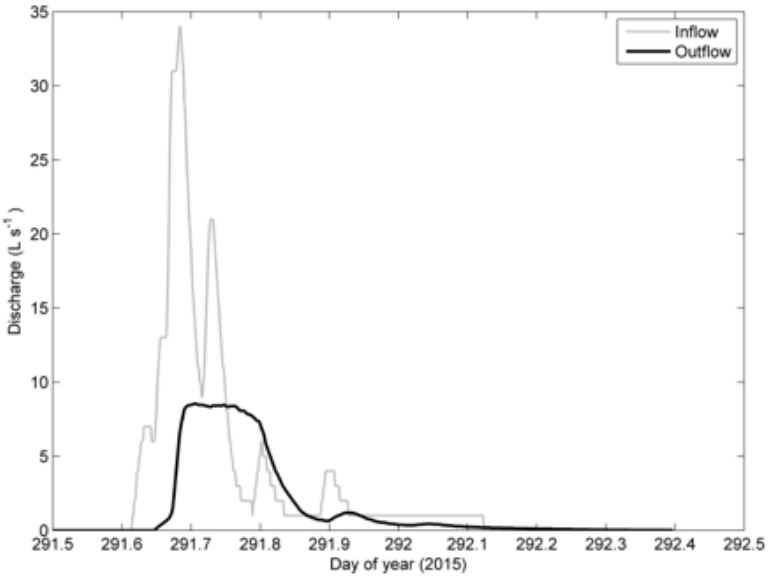

Figure 43: Event on 18 October. Total rainfall of 11.6 mm.

Appendix 2 – Box plots of concentration data

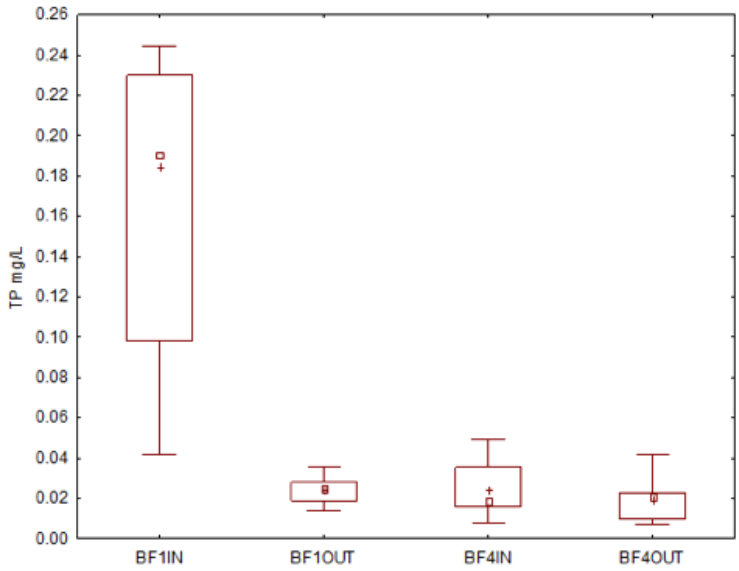

Figure 44: Total phosphorus concentration for inflow and outflow data corresponding to the raingarden and bioretention basin. Median (□), mean (+), whisker 25-75% percentile range (box), and non-outlier range (whiskers).

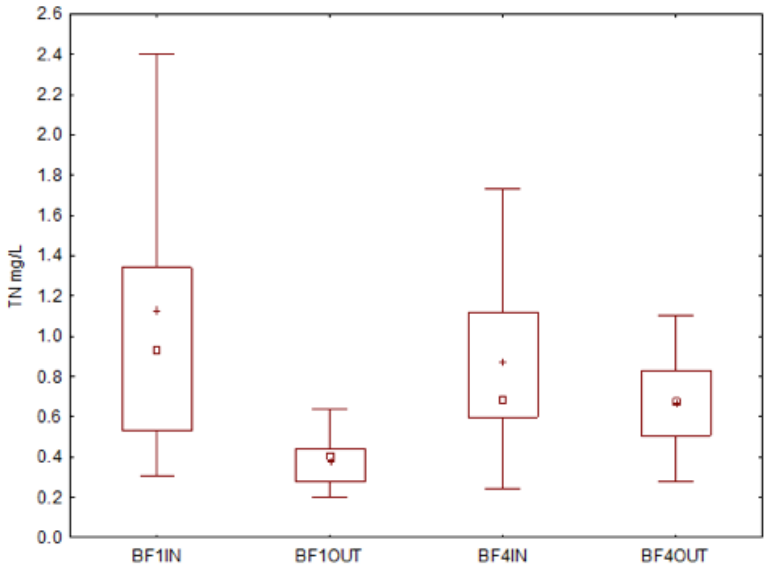

Figure 45: Total nitrogen concentration for inflow and outflow data corresponding to raingarden and bioretention basin. Median (□), mean (+), whisker 25-75% percentile range (box), and non-outlier range (whiskers).

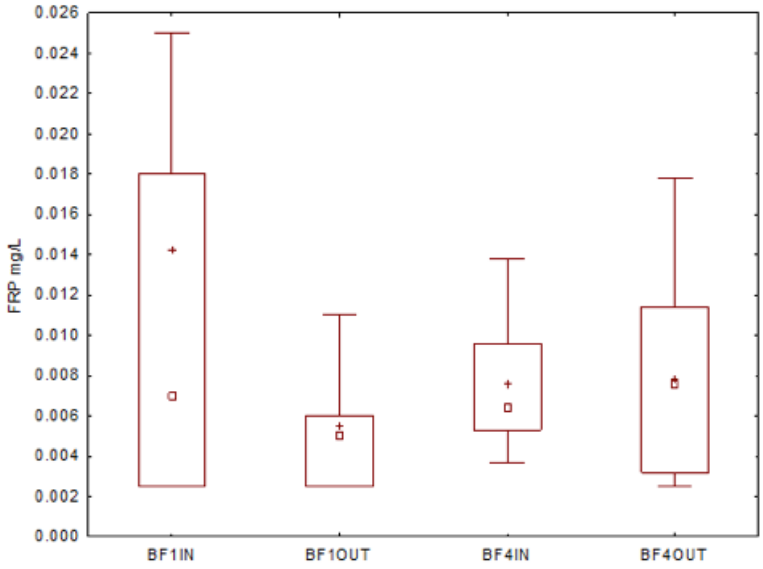

Figure 46: Filterable reactive phosphorus concentration for inflow and outflow data corresponding to raingarden and bioretention basin. Median (□), mean (+), whisker 25-75% percentile range (box), and non-outlier range (whiskers).

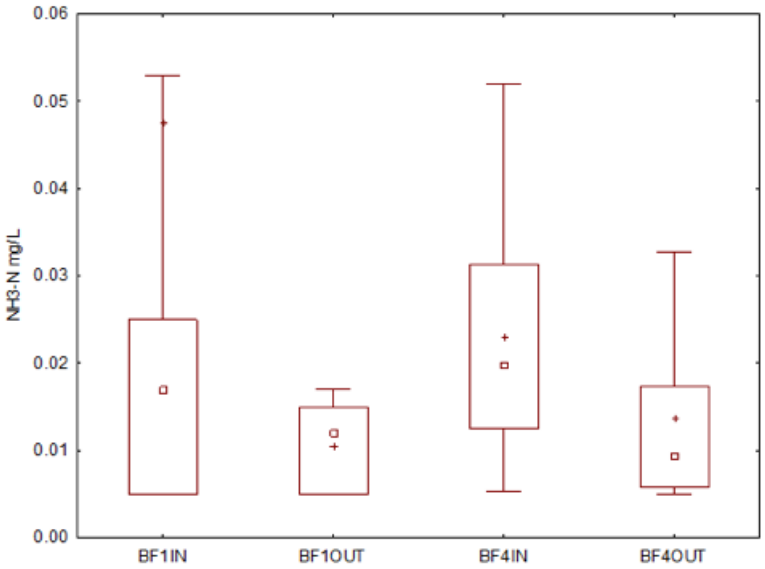

Figure 47: Ammonia-nitrogen concentration for inflow and outflow data corresponding to raingarden and bioretention basin. Median (□), mean (+), whisker 25-75% percentile range (box), and non-outlier range (whiskers).

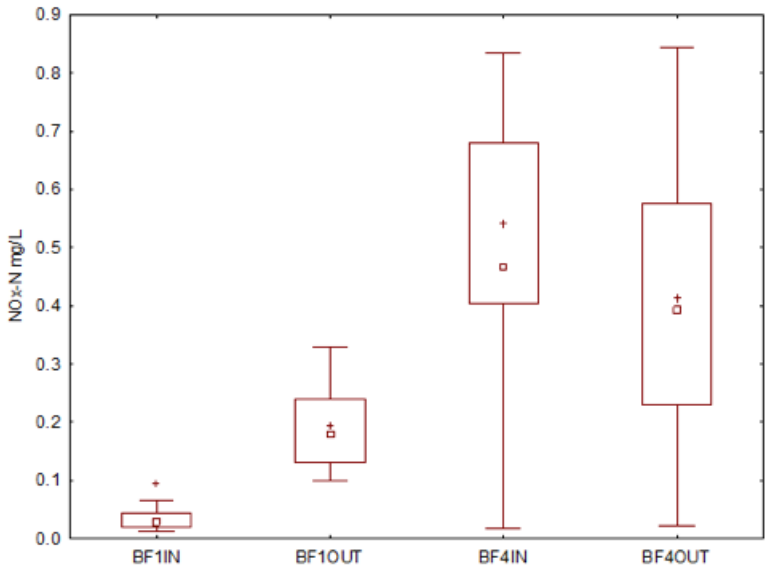

Figure 48: Nitrate-nitrogen concentration for inflow and outflow data corresponding to raingarden and bioretention basin. Median (□), mean (+), whisker 25-75% percentile range (box), and non-outlier range (whiskers).

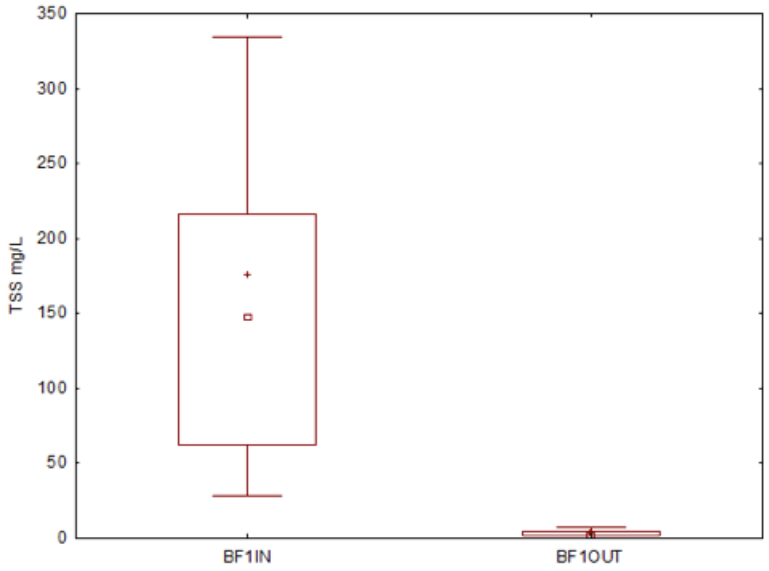

Figure 49: Total suspended solid concentration for inflow and outflow data corresponding to raingarden. Median (□), mean (+), whisker 25-75% percentile range (box), and non-outlier range (whiskers).

Appendix 3 – Additional photographs

Figure 50: Event on 22 July at BF1 pit. Source D. Sidoti (2015).

Figure 51: Event on 22 July at bioretention basin inflow station (BF4IN). Source D. Sidoti (2015).

Figure 52: Event on 22 July at bioretention basin storage (BF4STOR). Source D. Sidoti (2015).

Figure 53: Event on 22 July at bioretention basin outflow (BF4OUT). Discharge from subsurface pipes at a flow rate of 12 L/s. Source D. Sidoti (2015).

Figure 50: Event on 22 July at BF1 pit. Source D. Sidoti (2015).

Cooperative Research Centre for Water Sensitive Cities

Level 1, 8 Scenic Boulevard
Monash University
Clayton VIC 3800

info@crcwsc.org.au

www.watersensitivecities.org.au